

# A STUDY OF YAGI-UDA ANTENNA

By  
S JAGANNATHAN

EE  
1980  
M  
JAG

TH  
EC/1952/11  
J 18/5



DEPARTMENT OF ELECTRICAL ENGINEERING  
STU INDIAN INSTITUTE OF TECHNOLOGY, KANPUR  
JUNE, 1980

# A STUDY OF YAGI-UDA ANTENNA

A Thesis Submitted  
In Partial Fulfilment of the Requirements  
For the Degree of  
MASTER OF TECHNOLOGY

By  
S JAGANNATHAN

to the  
DEPARTMENT OF ELECTRICAL ENGINEERING  
INDIAN INSTITUTE OF TECHNOLOGY, KANPUR  
JUNE, 1980

I - V / DIR  
CEN  
PARTY  
App. No. A 63791

20 NOV 1980

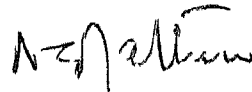
EE-1980-M-JAG-STL'

## ABSTRACT

This thesis makes a study of "Yagi-Uda Antenna". The design of an Yagi array, given the gain, array size and percentage bandwidth is given. A study of current distribution in the elements of the Yagi, by Moments Method and also by King's method is explained. The procedure for calculation of current distribution, gain, input impedance and directivity by King's method are given. A computer program was prepared, which analyzes the Yagi by King's method. Experimental set ups were used to measure the performance. The computed results are compared with earlier published results and with experimental measurements.

CERTIFICATE

It is certified that this work entitled  
'A Study of Yagi-Uda Antenna' by S Jagannathan  
has been carried out under my supervision and  
that this work has not been submitted else where  
for a degree.



( N.C. MATHUR )  
Professor  
Department of Electrical Engineering  
Indian Institute of Technology  
KANPUR

## ACKNOWLEDGEMENT

I wish to take this opportunity to express my deepest sense of gratitude to my supervisor Dr N.C. Mathur who provided me the much needed infalliable guidance. His sincere advice and keen interest during the course of this work has been a source of constant encouragement to me.

I am very much grateful to my friend Shri Rakesh Chadha for his constant inspiration, untiring help and useful discussion from time to time without which this work would not have been in the present shape. Thanks are also due to my friends Shri Meenakshi Sundaram and Shri Karuppasamy whose help in conducting the experiments on the Western Laboratory terrace of IIT Kanpur was invaluable I also thank Shri Arunachalam and Shri Ramachandran for their unstinted help and guidance.

Also, I would like to thank the staff members of the Electrical Engineering, IIT Kanpur for their invaluable cooperation and for providing facilities for the successful completion of this work.

Special thanks are due to Mr. Rawat (Typing), Mr. Ganguli (Figures) and Mr Triveni Tiwari (Cyclostyling).

- S. Jagannathan

## TABLE OF CONTENTS

Chapter	Title	Page
	Abstract	iii
	Acknowledgement	iv
	List of Figures	vi
1	Introduction	1
2	Design of Yagi-Uda Antenna	8
3	Analysis of Yagi Antenna by Moments Method	12
4	Analysis of Yagi Antenna by King's Method	25
5	Computations for Pattern, Gain and Impedance	52
6	Antenna Measurements	61
7	Results and Discussions	76
	Appendix I - Design Tables	88
	Appendix II- Two elements	91
	Appendix III- Computer Programme	101
	List of References	112
	Photos of Transmitter and Receiver.	

## LIST OF FIGURES

Sl.No	Fig No	Title	Page
1	1.1	A Typical Yagi-Uda Array	3
2	2 1	The Relationships between Array size, Bandwidth and Directivity	10
3.	3.1	Coordinate system used to analyze Yagi-Uda array	17
4	3 2	Diagram showing distance from a matching point on pth&on qth element	19
5.	3.3	Parasitic element with N-Matching points along its axis	21
6	3 4	Driven element with N-1 matching points along its axis	21
7	4 1	Base driven Monopole over perfectly conducting ground screen	27
8.	4.2	The functions $\frac{\sin\beta_o R}{\beta_o R}$ , $\frac{\cos\beta_o R}{\beta_o R}$ and $\frac{\cos\beta_o R}{2}$	33
9	5.1	Antenna and coordinates for pattern measurement	54
10.	5.2	Coordinate system for calculations in the Farzone	55
11	5.3	Coordinates for 4 element array	58
12.	6.1	Balun construction	63
13.	6.2	Impedance Measurement	64
14	6.3	Impedance Measurement using Smith Chart	66
15.	6.4	Phase difference between centre and edges of receiving array	69



Sl No	Fig No.	Title	Page
16	6.5	Gain Measurement	70
17	6.6	Folded dipole	72
18	6 7	Mast	73
19	6 8	Physical layout of the Yagi antenna	74
20	7 1	Current distribution in Yagi antenna with initial arrangement	79
21	7 2	E-Field pattern of Yagi-Uda Antenna	80
22.	7.3	Comparison of initial, space perturbed and optimum patterns	83
23	7.4	Bandwidth of antenna	84
24	7 5	Gain vs No of elements	87
25	A 1	Two identical parallel elements	92
26.	A.2	The functions $S_p(h-\angle)-S_p(h,h)$ compared with three trigonometric functions	99

## CHAPTER 1

### INTRODUCTION

#### 1.1 General

Antennas are basic components of any electrical communication system which depends on free space as a propagating medium. The antenna is the connecting link between free space and the transmitter or receiver. In many systems for navigational or direction-finding purposes, the operational characteristics of the system are designed around the directive properties of the antenna. In other systems, the antenna may be used simply to radiate energy in an omnidirectional pattern in order to provide a Broadcast type of coverage. In still other systems, the antenna may have a highly directional pattern to achieve increased gain and reduced interference.

A general broadcast receiver antenna must have the following properties: Low cost, simplicity of construction and erection, low wind resistance, low sensitivity to small shifts in position and must require least maintenance. This is because the users are mostly non technical people. Television channels fall in the very High Frequencies (VHF) and Ultra High Frequencies (UHF) bands. Since VHF and UHF signals decay rapidly with distance, TV receiving antennas are required to have a high gain, particularly in fringe areas.

Yagi-Uda antenna fits the bill adequately in all respects. Its structure has low wind resistance and its beamwidth is sufficiently large to take care of small shifts in position, due to wind, rain, birds etc. It has a gain in the range of 8 to 13 dB over a simple dipole and the construction does not involve any costly machining process. Yagi's are used in Radio astronomy applications also

A conventional Yagi array consists of a row of parallel straight cylindrical dipoles of which only the second one is driven by a source and all others are parasitic. The driven element is approximately half a wave length long and is usually the second in number. The first element is slightly longer than half a wavelength and is known as reflector. The remaining elements are known as directors which are shorter than the driven element. Figure 1.1 shows the parameters of a Yagi antenna.

The properties of an antenna which are most often of interest are the radiation pattern, gain and impedance. In this thesis these aspects of Yagi antenna are studied

## 1.2 Outline of the work

This chapter gives an introduction to the subject and presents a literature survey on Yagi antennas. Chapter 2 explains the design of Yagi antenna given some specification

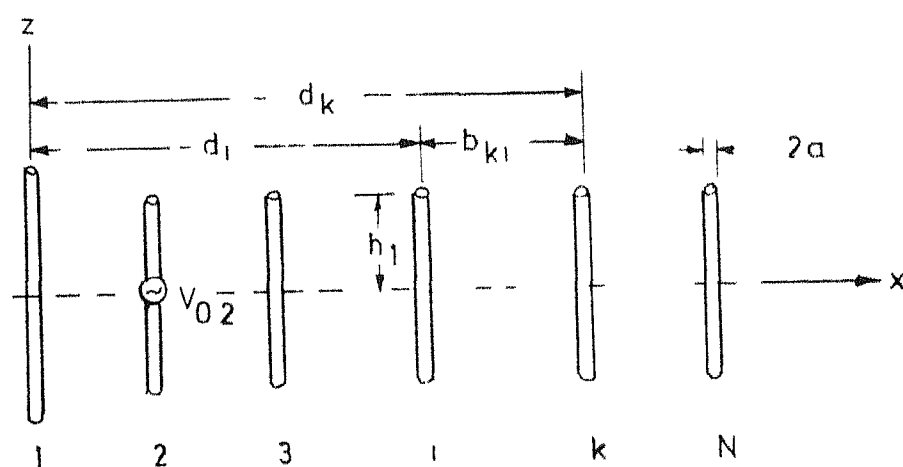


FIG 11 A TYPICAL YAGI-UDA-ARRAY  
 1 REFLECTOR  
 2 DRIVEN ELEMENT  
 3-N DIRECTORS

like Directivity, Bandwidth, array size etc Tables given in the Appendix I aid the design. Chapter 3 presents an analysis of this antenna by Moments method. Computer techniques more than analytical discussions is the important difference between this method and the King's three term current theory described in the next chapter (4) King's method, unlike his predecessor's, follows an analytical approach to the formulation of the current expression. His matrices are of a smaller order and hence subsequent computer work is comparatively simple

Chapter 5 explains the computations involved in finding the characteristics of the antenna like Input Impedance, Gain, Directivity and Field Pattern. Chapter 6 gives the actual experimental set up for the above measurements Since the author wanted to verify the claims made by Cheng and Chen (17) about increased directivity with optimization of elements, the antenna built, conforms to their design specifications Chapter 7 presents a discussion on the results obtained A computer listing appears in the Appendix II which will aid any further work on this antenna

### 1.3 Literature Survey

From a recent paper by Kahn (1), it is confirmed now that Prof Uda of Tohoku Imperial University, Japan invented the Yagi-Uda array (2) in the year 1926 However as Yagi,

a colleague of Prof Uda, published a paper in English (3) in 1928, in which he first mentioned the array, the antenna was known as 'Yagi array' Now it is called rightly as 'Yagi-Uda array'

In 1946 Walkinshaw (4) computed and plotted a large number of directive polar diagrams for several shortend-fire arrays with a driven half wave dipole and a maximum of four half wave parasitic elements Reid (5) and Fishenden and Wiblin (6) analysed the array but their assumption that equal currents flow in all directors was wrong. Reid considered the array as a continuous arrangement of very short dipoles Fishenden and Wiblin considered only half wave elements with sinusoidal current distribution.

Dhrenspeck and Poehler (7) investigated experimentally and systematically a method for obtaining maximum gain from a Yagi-Uda array with equally spaced directors of equal length They concluded that the phase velocity of the surface wave travelling along the row of directors could be used as a design criterion The phase velocity depends on the element length and spacing parameters in a complicated way The surface wave concept has also been used by various authors to calculate the phase velocity of infinitely long uniform dipole arrays with assumed current distributions (8), (9) to determine the cut off frequencies (10) and to analyze infinite and semi-infinite Yagi-Uda

arrays (11), (12) An approximate method for studying the behaviour of finite arrays by matching the terminal Zone solutions of semi-infinite arrays was discussed by Maillour (12)

To maximize gain the antenna parameters e g inter-element spacing, length of the elements and diameter of the elements must be optimized This approach is found in Bojsen et al (13), Morris (14), Tseng and Cheng (15) and Cheng and Chen (18), (19) papers Bojsen's results dispute the travelling wave theory But he neglected the dipole radius and assumed sinusoidal current distributions. Morris used an arrangement in which the driven element was a half wave dipole ( $2h_2 = \lambda/2$ ) and the single reflector ( $2h_1 = 0.51\lambda$ ) was placed at a quarter wavelength behind the driven element ( $b_{12} = 0.25\lambda$ ) This gave a high forward gain He plotted curves showing the variation of gain with inter-element spacing. His conclusion that if the interelement spacing is longer than ( $0.4\lambda$ ), the gain will fall concurs with the findings of Ehrenspeck and Poehler (7)

Cheng and Chen used a three term approximation for current, developed by King et al (16) They maximized gain by optimizing interelement spacing (18) and element length (19) Kajfez found that nonlinear optimization reduces the side lobes of Yagi antenna (22)

Shen gave a numerical approach (21) for the design of Yagi antenna (20) Thiele (24) and Lakla (23) also have contributed for the analysis of Yagi array.

Thiele (27) and Harrington (17) have explained the moments method solution for current and field problems of Yagi array.



## CHAPTER 2

### DESIGN OF YAGI-UDA ANTENNA

#### 2 1 General

In this chapter the theoretical constraints on the parameters of the Yagi-Uda antenna are given. Also the design of an Yagi array, given a set of specifications like Directivity, Bandwidth etc is indicated. The Tables given in the Appendix I aid the design.

#### 2 2 Theoretical Constraints

The parameters of the Yagi antenna are the number of elements, the length of the elements, the radius of the elements and the spacing between the elements.

In King's (16) 3 term current theory, the assumptions  $\beta_0 b \gg 1$  and  $\beta_0 h_1 \leq 5\pi/4$  are made to satisfy some conditions. Here  $\beta_0 (= 2\pi/\lambda)$  is the free space wave number and  $\lambda$  is the wavelength, 'b' is the inter-element spacing and  $h_1$  is the half element length of the 1th conductor in the array. Also  $\beta_0 a \ll 1$  where 'a' is the radius of the elements.

Fishenden and Wiblin (6) stipulated that the length of the array should not exceed  $6\lambda$  and 'b' should be  $\lambda/3$ . Poehler (7) Morris (14) and Cheng and Chen (18) found both theoretically and experimentally that the spacing between the reflector and the driven element, if kept equal to

$0.25\lambda$  gives a maximum gain. Also the Reflector should be  $0.51\lambda$  long. Inter director spacing must be less than  $0.4\lambda$ .

Cheng and Chen found that in practice if the length of the driven element is slightly less than  $0.5\lambda$ , the gain is increased.

The Bandwidth of an array is defined as the frequency range in which the directivity falls to 3 dB less than the maximum directivity value. According to Shen (20) the bandwidth of an Yagi array is limited to the bandwidth of the pass bands of the travelling wave Yagi array is supposed to support a travelling wave since it radiates primarily in the end fire direction. The pass bands are bounded by the upper and lower cut off frequencies ( $\beta_0 h$  is essentially a frequency term). The upper cut off frequency can be found by a rigorous mathematical analysis of the structure (28). The lower limit is determined by the requirement that the power density should decay at least as fast as  $\exp(-r/h)$  where 'r' is the distance measured from the centre of the array to a point in the transverse direction. The three pass bands are

$$\left. \begin{array}{l} K_h = 0 \text{ to } 1.57 \\ K_h = 4.49 \text{ to } 4.71 \\ \text{and } K_h = 7.73 \text{ to } 7.85 \end{array} \right\} K_b < 3.14$$

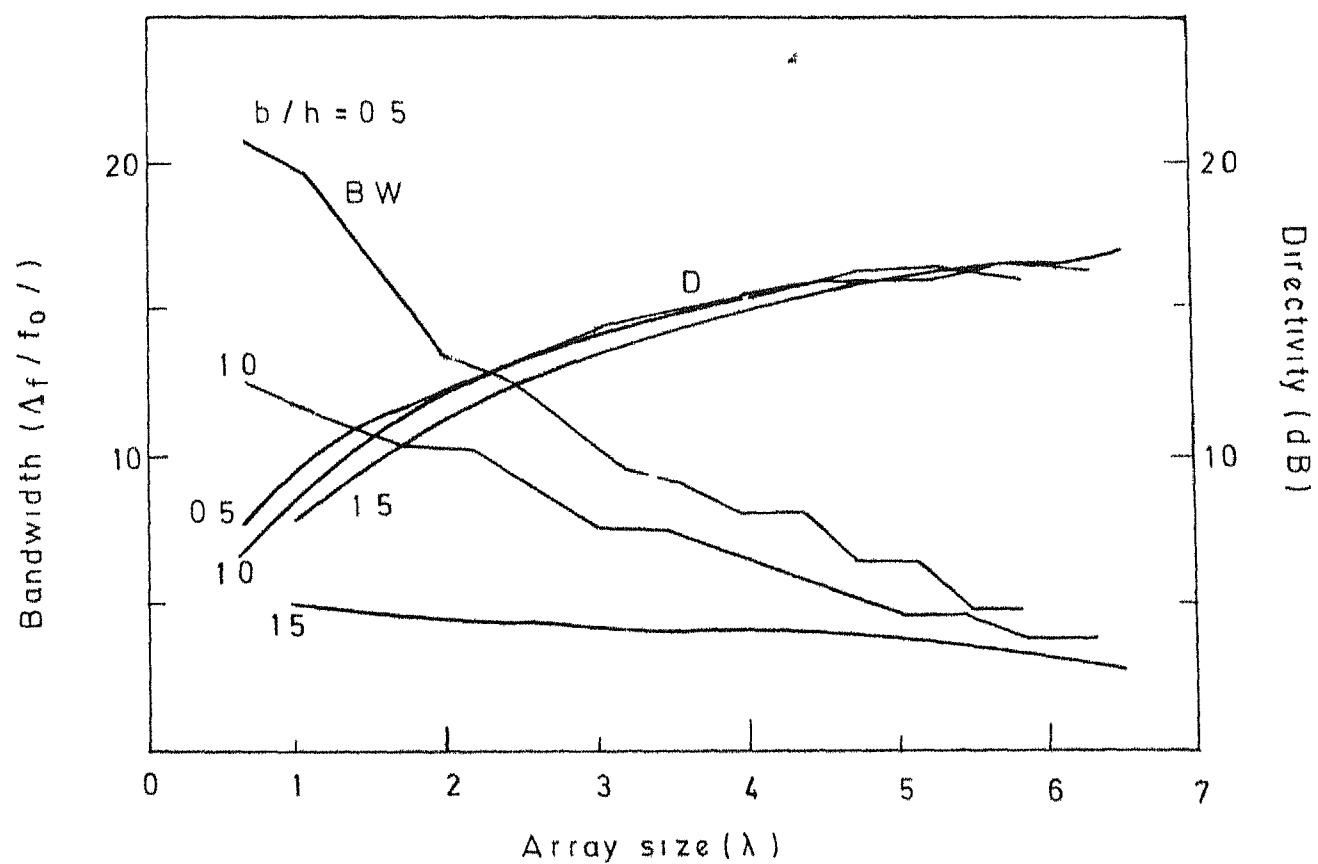


FIG 21 THE RELATIONSHIPS BETWEEN ARRAY SIZE , BAND - WIDTH AND DIRECTIVITY [from Shen(20)]

### 2.3 Design of an Yagi array

Shen (7) has indicated a procedure by which, given the central frequency, required Bandwidth and the length of the array, we can design an Yagi antenna which would have maximum directivity and minimum number of elements. The design constraints were that the central frequency should be 200 MHz ( $\lambda = 1.5$  m) and the bandwidth approximately 10%. The length of the array should be 3 metres

The length of the array being  $2\lambda$  and the Bandwidth 10%, we chose curve 'b' where  $\frac{b}{h} = 1.0$  for our design in Figure 2.1. This gives a directivity of approximately 12 dB. Now referring to Table (II) <sup>in Appendix I</sup> which pertains to  $\frac{b}{h} = 1$ , we can see that, if the number of parasitic elements is equal to 9, we get a directivity of approximately 12 dB with 10.3% bandwidth. The  $\beta_{oh}$  value 1.36 determines the length of the directors approximately as 0.65 m. As  $\frac{b}{h} = 1$ , the spacing between the elements = 0.324 m. We can take  $\frac{a}{h} = 0.01$  and then  $a = 0.0032$  m. The array length will be  $1.96\lambda$  or 2.94 m. The array will have one reflector, one driven element and eight directors.

### 2.4 Conclusion

With the help of the graph and the tables we can <sup>with</sup> design any array even/only two out of the three constraints namely Bandwidth, Directivity or array size given.

## CHAPTER 3

### ANALYSIS OF YAGI ANTENNA BY MOMENTS METHOD

#### 3.1 General

High speed digital computers have simplified the job of the antenna engineers in that numerical techniques can be used where analytical solutions are not available. It is now possible with the aid of approximation techniques to get very accurate results about antenna performance with the aid of computers.

Field computations by Moments Method was first introduced by Harrington (17) Thiele (27) solved the Yagi antenna problem using Moments method In his work Matrix methods are used largely in solutions to field problems. The basic idea is to reduce a functional equation to a matrix equation by known techniques

#### 3 2 Method of Moments

Let us see a general procedure for solving linear equations, called the method of moments. Consider the inhomogeneous equation

$$L(f) = g \quad (3.1)$$

where 'L' is an operator, 'g' is the source or excitation (known function) and 'f' is the field or response (unknown function to be determined) We are interested

in an unique solution Let 'f' be expanded in a series of functions  $f_1, f_2, f_3 \dots$  in the domain of L as

$$f = \sum_n \alpha_n f_n \quad (3.2)$$

where the  $\alpha_n$  are constants. We shall call the  $f_n$  expansion functions or basis functions. For exact solutions (3.2) is an infinite summation and  $f_n$  form a complete set of basis functions. For approximate solutions, however, (3.2) is a finite summation. Substituting (3.2) in (3.1) and using the linearity of L, we have

$$\sum_n \alpha_n L(f_n) = g \quad (3.3)$$

It is assumed that a suitable inner product  $\langle f, g \rangle$  has been determined for the problem. Defining a set of weighting functions or testing functions,  $w_1, w_2, w_3 \dots$  in the range of L, and taking the inner product of (3.3) with each  $w_m$  we get

$$\sum_n \alpha_n \langle w_m, L f_n \rangle = \langle w_m, g \rangle \quad (3.4)$$

$m = 1, 2, 3, \dots$  This set of equations can be written in matrix form as

$$[l_{nm}][\alpha_n] = [g_m] \quad (3.5)$$

where

$$[l_{mn}] = \begin{bmatrix} \langle w_1, L f_1 \rangle & \langle w_1, L f_2 \rangle & \dots \\ \langle w_2, L f_1 \rangle & \langle w_2, L f_2 \rangle & \dots \\ \dots & \dots & \dots \end{bmatrix} \quad (3.6)$$

$$[\alpha_n] = \begin{bmatrix} \alpha_1 \\ \alpha_2 \\ \vdots \end{bmatrix} \quad [g_m] = \begin{bmatrix} \langle w_1, g \rangle \\ \langle w_2, g \rangle \\ \vdots \end{bmatrix} \quad (3.7)$$

If the matrix  $[l]$  is nonsingular its inverse  $[l^{-1}]$  exists. The  $\alpha_n$  are then given by

$$[\alpha_n] = [l_{mn}^{-1}] [g_m] \quad (3.8)$$

and the solution for  $f$  is given by (3.2). Defining the matrix of functions,

$$[f_n] = [f_1, f_2, f_3, \dots] \quad (3.9)$$

we write,

$$[f] = [f_n^v] [w_n] = [f_n] [l_{mn}^{-1}] [g_m] \quad (3.10)$$

This solution may be exact or approximate depending upon the choice of the  $f_n$  and  $w_n$ . The choice  $w_n = f_n$  is known as Galerkin's method.

One of the main tasks in any particular problem is the choice of the  $f_n$  and  $w_n$ . The  $f_n$  should be linearly independent and chosen so that some superposition (3.2) can approximate  $f$  reasonably well. The  $w_n$  should also be linearly independent and chosen so that the product  $\langle w_n, g \rangle$  depend on relatively independent properties of  $g$ . Additional factors which affect the choice of  $f_n$  and  $w_n$  are

1. the accuracy of solutions desired
2. the ease of evaluation of the matrix elements
- 3 the size of the matrix that can be inverted
4. the realization of a well conditioned matrix [1]

The integration involved in evaluating the  $I_{mn} = \langle w_m, f_n \rangle$  of (3.6) is often difficult to perform in problems of practical interest. A simpler way to get approximate solutions is to require that equation (3.3) be satisfied at discrete points in the region of interest. This procedure is called point-matching method.

There are two types of Basis function used in Moments Method. The Entire domain Basis function is defined and non-zero over the entire domain. Examples are Fourier, Chebyshev, Maclaurin and Legendre series. The other types are sub-domain bases, which exist in the domain of  $L_{op}$ , but are zero over part of that domain. Examples are triangle functions, quadratic interpolations etc.

### 3.3 Application to the Yagi-Uda Antenna

Thiele has analysed Yagi-Uda antenna using Moments method. He used a current generator as a source on the driven element. Entire domain Basis function and Point matching techniques were used.



Fig 3 1 shows the coordinate system used to analyze Yagi-Uda array To find  $L_{op}$  in

$$L_{op} ( J ) = (E^1) \quad (3.11)$$

where  $J$  is the current density and  $E^1$  is the incident electric field We consider the various elements in the array as individual wire antennas. It can be shown that the operator for the  $p$ th element is

$$L_{op} = \frac{-\lambda \sqrt{\mu/\epsilon}}{8 \pi^2 a} \int_{-L_p/2}^{L_p/2} G(r, r') dz' \quad (3.12) \quad dz$$

is a good choice (27) Here

$$G(r, r') = \frac{\exp(-jkr)}{r^5} \left[ (1+jkr)(2r^2-3a^2) + k^2 a^2 r^2 \right] \quad (3.13)$$

$$\text{and } r = \sqrt{(X'-X)^2 + (Y'-Y)^2 + (Z'-Z)^2 + a^2} \quad (3.14)$$

Since we are considering each element in the array to be an individual wire antenna let us use the entire domain basis functions

The current  $J_p(Z)$  on the  $p$ th element is assumed to be uniform along the circumference Thus

$$J_p(Z) = 2 \pi a I_p(Z) \quad (3.15)$$

We expand  $I_p(Z)$  in terms of entire domain basis function   
 (Fourier)   
 as follows

$$I_p(Z) = \sum_{n=1}^N I_{n_p} \cos(2n-1) \frac{\pi Z}{L_p}, \quad -\frac{L_p}{2} \leq Z \leq \frac{L_p}{2} \quad (3.16)$$

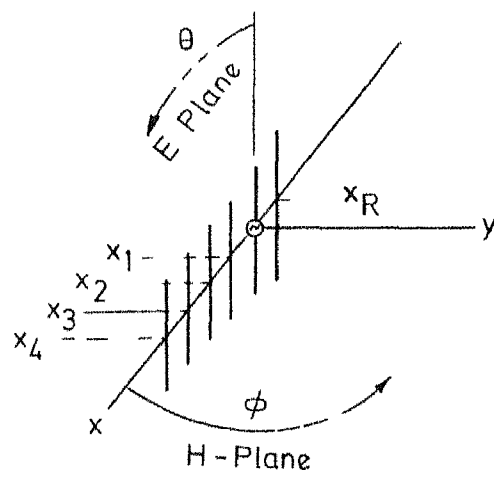


FIG 31 COORDINATE SYSTEM USED TO ANALYZE  
YAGI UDA ARRAY

The operator  $L_{op}(J)$  must be evaluated not only when the observation point is on element  $p$ , but also when it is on the other elements as well, as indicated in Fig. 3.2. Thus we can write

$$L_{op}(J) = \frac{-\lambda \sqrt{\mu/\epsilon}}{8\pi^2 j} \sum_{p=1}^{D+2} \sum_{n=1}^N I_{n_p} \int_{-L_p/2}^{L_p/2} G(r, r') \cos(2n-1) \frac{\pi z'}{L_p} dz' \quad (3.17)$$

where  $(D+2)$  represents the total number of elements in the Yagi-Uda array ( $D$ =number of directors) and  $N$  is the number of entire domain basis functions retained on each element in the array. The entire field radiated by the array is represented by (3.17).

In an array composed of a reflector a driven element and  $D$  directors, let us assume that there will be  $N$  modes on each element and let each element be of different length. Using (3.17), the first part of the system of equations is then of the form

$$\sum_{p=1}^{D+2} \sum_{n=1}^N Z_{m,n_p} I_{n_p} = 0, \quad m = 1, 2, \dots, N \times D \quad (3.18)$$

where

$$Z_{m,n_p} = \frac{\lambda \sqrt{\mu/\epsilon}}{8\pi^2 j} \int_{-L_p/2}^{L_p/2} G(r, r') \cos(2n-1) \frac{\pi z'}{L_p} dz' \quad (3.19)$$

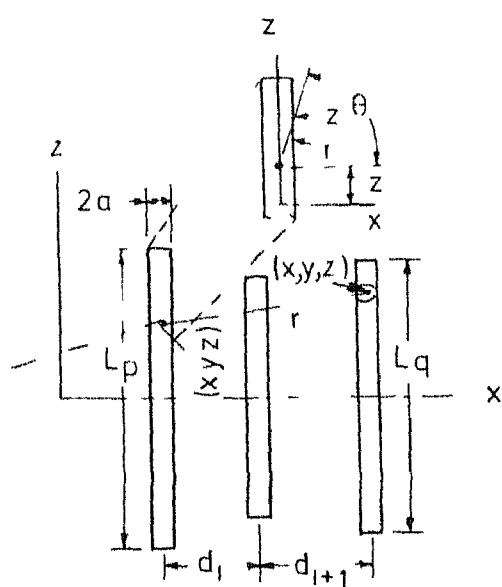


FIG 3 2 DIAGRAM SHOWING DISTANCE FROM A MATCHING POINT ON  $p$ th ELEMENT TO SOURCE REGION ON  $q$ th ELEMENT  
 INSERT SHOWS RELATIONSHIP BETWEEN  $z'$  AND  $\theta$  WHEN OBSERVATION POINT AND SOURCE REGION ARE ON THE SAME ELEMENT

These equations are generated by requiring that the tangential E field be zero at N points on each director Or  $E^{\text{tan}}$  is zero at  $N \times D$  points on the directors The matching points on a director are shown in Fig 3 3

The next N equations are similar to the previous  $N \times D$  equations since tangential E vanishes at N points on the reflector element, as shown in Fig 3 3 Thus

$$\sum_{p=1}^{D+2} \sum_{n=1}^N Z_{m,n_p} I_{n_p} = 0, \quad m = (N \times D) + 1, \quad N \times (D + 1) \quad (3.20)$$

The last N equations are generated by using the boundary condition on the driven element as shown in Fig 3.4. That is

$$\sum_{p=1}^{D+2} \sum_{n=1}^N Z_{m,n_p} I_{n_p} = 0, \quad m = N \lambda (D+1) + 1, \quad N \lambda (D+2) - 1 \quad (3.21)$$

and for the driven element at the driving point

$$\sum_{n=1}^N I_{n_e} = 1, \quad e = D+2, \quad m = N \lambda (D+2) \quad (3.22)$$

On the driven element the tangential E boundary condition is only enforced at  $N-1$  points even though there are N modes The Nth equation on the exiter arises from the constraint on the terminal current value.

In equation (3.11) we have set  $(E^1)$  to zero as no incident field is considered in this formulation Let us

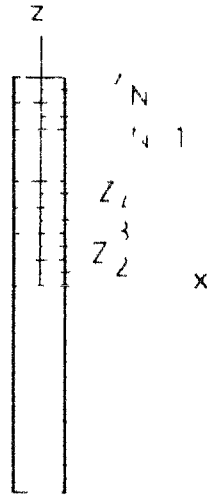


FIG 3 3 PARASITIC ELEMENT WITH  $N$ -MATCHING POINTS ALONG ITS AXIS

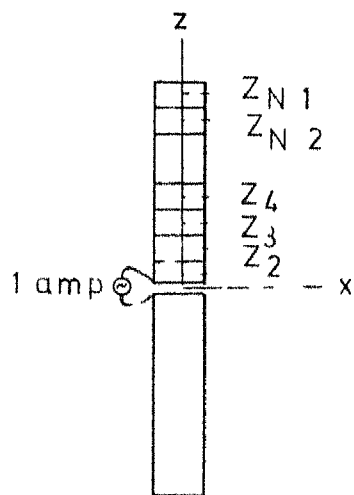


FIG 3 4 DRIVEN ELEMENT WITH  $N + 1$  MATCHING POINTS ALONG ITS AXIS

consider an example given by Thiele in which one reflector, one driven element and one director are present. Assuming that only two modes are present in each element, we get

$$\begin{bmatrix} Z_{11} & Z_{12} & Z_{13} & Z_{14} & Z_{15} & Z_{16} \\ Z_{21} & Z_{22} & Z_{23} & Z_{24} & Z_{25} & Z_{26} \\ Z_{31} & Z_{32} & Z_{33} & Z_{34} & Z_{35} & Z_{36} \\ Z_{41} & Z_{42} & Z_{43} & Z_{44} & Z_{45} & Z_{46} \\ Z_{51} & Z_{52} & Z_{53} & Z_{54} & Z_{55} & Z_{56} \\ 0 & 0 & 1 & 1 & 0 & 0 \end{bmatrix} \begin{bmatrix} I_1 \\ I_2 \\ I_3 \\ I_4 \\ I_5 \\ I_6 \end{bmatrix} = \begin{bmatrix} 0 \\ 0 \\ 0 \\ 0 \\ 0 \\ 1 \end{bmatrix} \quad (3.23)$$

That is at point  $Z_1$  on element 1 (the reflector),  $Z_{11}$  is the "field" generated by mode 1, and  $Z_{12}$  is the field generated at the same point by mode 2.  $Z_{21}$  is the field generated by mode 1 at point  $Z_2$  on the reflector and  $Z_{22}$  is that of mode 2. Similarly we can explain  $Z_{33}$ ,  $Z_{34}$ ,  $Z_{43}$  and  $Z_{44}$ .

If we write (3.23) in a submatrix form,

$$\begin{bmatrix} S_{11} & S_{12} & S_{13} \\ S_{21} & S_{22} & S_{23} \\ S_{31} & S_{32} & S_{33} \end{bmatrix} \begin{bmatrix} I_1 \\ I_2 \\ I_3 \\ I_4 \\ I_5 \\ I_6 \end{bmatrix} = \begin{bmatrix} 0 \\ 0 \\ 0 \\ 1 \\ 0 \\ 0 \end{bmatrix} \quad (3.24)$$

then it is clear that regardless of the number of submatrices, those on the main diagonal of submatrices ( $S_{11}$   $S_{22}$ ,  $S_{33}$ ) will represent the field generated by the current on the element at which the tangential E boundary condition is being enforced. Hence if there are D identical directors the last D submatrices on the main diagonal will all be identical.

For elements off the main diagonal of submatrices the explanation is as follows. The quantity  $Z_{35}$  represents the field at a point 1 on element 2 (the driven element) due to the first mode (mode 5) on the director (element 3). Similarly  $Z_{36}$ ,  $Z_{45}$  and  $Z_{46}$ . Thus submatrices  $S_{qr}$ ,  $q \neq r$ , represent the interaction between elements q and r. If all directors are of the same length then,  $S_{qr} = S_{rq}$  for director submatrices. Further for uniform director spacing there will be several interdirector spacings or distances that will be the same. If the directors are also of same length, then we need not calculate the director submatrices individually. Thus computation time is saved.

Once the current in the individual element are found by solving (3.24), the calculation of pattern, gain and impedance are very simple. The procedure is explained in Chapter 5.



### 3.4 Conclusion

As Cheng and Chen (13) pointed out, in subsectioning the array elements, matrices of much larger dimension would have to be manipulated. Thiele, himself said that two modes per element is very inadequate and minimum three per parasitic elements and five modes for the driven element are needed for good results. This limits the number of array elements that can be handled. Furthermore, the currents on the parasitic elements depend much more critically upon those on other mutually coupled elements. The effects of small errors multiply and there would be convergence problems unless more subsections than those normally required for driven elements are taken.

In using the three term theory of King's, the largest matrices to be handled for an  $N$  element array are of a dimension  $N \times N$  and no convergence problems are encountered in optimizing the array for maximum gain. Hence in this work, King's three term theory is used for current distribution and the procedure is explained in the next chapter.

## CHAPTER 4

### ANALYSIS OF YAGI ANTENNA BY KING'S METHOD

#### 4.1 Three term current theory

King, Mach and Sandler (16) have formulated an alternative approach to the problem of finding current distribution in the elements of the Yagi-Uda antenna. They assumed a three term approximation for current which is given below (for the  $i$ th element)

$$I_{Z_1}(Z_1) = A_1 M_{O_{Z_1}} + B_1 F_{O_{Z_1}} + D_1 H_{O_{Z_1}} \quad (4.1)$$

$A_1 = 0$  for  $i \neq 2$ .  $A_2$ ,  $B_1$  and  $D_1$  are complex constants to be evaluated and

$$M_{O_{Z_1}} = \sin \beta_0 (h_1 - |Z_1|) \quad (4.2)$$

$$F_{O_{Z_1}} = \cos \beta_0 Z_1 - \cos \beta_0 h_1 \quad (4.3)$$

$$H_{O_{Z_1}} = \cos \frac{1}{2} \beta_0 Z_1 - \cos \frac{1}{2} \beta_0 h_1 \quad (4.4)$$

These three components have been given a physical explanation by King as follows  $M_{O_{Z_1}}$  is the simple sinusoid. This component of the current is maintained directly by the generator ( $V_{O2}$ , the driving voltage in the driven element number 2). It does not

include the components that are induced by coupling between different parts of the antenna. The currents induced by the interaction between charges moving in the more or less widely separated sections of the antenna appear in two parts. One of these the shifted cosine, is maintained by that part of the interaction that is equivalent to a constant field acting in phase at all points along the antenna. The other part the shifted cosine with half angle arguments is the correction that takes account of the phase lag introduced by the retarded instead of instantaneous interaction.

#### 4.2 The Integral Equation

Let us try to determine the integral equation for base driven monopole (Fig. 4.1) over perfectly conducting ground screen (which may be approximated to a cylindrical dipole). We have the boundary conditions  $E_z(z) = 0$ , on the surface  $\rho = a$  of the perfectly conducting antenna.

From Maxwell Lorentz equations we know that for time dependent fields

$$\nabla \times \vec{B} = \mu_0 (\vec{J} + j\omega\epsilon_0 \vec{E}) \quad (4.5)$$

$$\nabla \cdot \vec{B} = 0 \quad (4.6)$$

$$\nabla \times \vec{E} = -j\omega\vec{B} \quad (4.7)$$

$$\nabla \cdot \vec{E} = \rho/\epsilon_0 = 0 \quad (4.8)$$

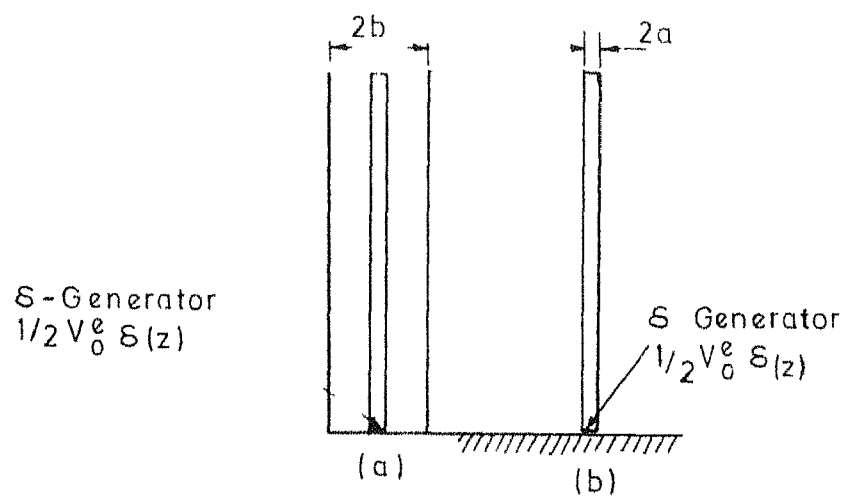


FIG 4 1 (a) COAXIAL LINE TERMINATED IN OPEN END  
 (b) BASE DRIVEN MONOPOLE OVER PERFECTLY  
 CONDUCTING GROUND SCREEN

which govern the interaction of charges and currents on conductors in space. A convenient method of solving the vector partial differential equations (4.5-4.8) is with the use of scalar and vector potentials  $\phi$  and  $\underline{A}$ . It is well known that the fields are derived from the vector potentials by the following equations

$$\underline{B} = \nabla \times \underline{A} \quad (4.9)$$

$$\text{and } \underline{E} = -\nabla\phi - j\omega\underline{A} \quad (4.10)$$

If we substitute (4.9) and (4.10) in the Maxwell's Equations we get mixed vector equations for  $\underline{A}$  and  $\phi$ . The variables can be separated if the following conditions relating  $\underline{A}$  and  $\phi$  are imposed.

$$\nabla \cdot \underline{A} = \frac{-j\beta_0^2}{\omega} \phi \quad (4.11)$$

This is known as the Lorentz condition. The resulting vector Helmholtz equations for  $\underline{A}$  and  $\phi$  in air are

$$(\nabla^2 + \beta_0^2) \underline{A} = -\mu_0 \underline{J} \quad (4.12)$$

$$(\nabla^2 + \beta_0^2) \phi = -\rho/\epsilon_0 = 0 \quad (4.13)$$

As we consider thin cylindrical conductors all aligned in the Z direction, we see that the boundary condition  $E_z(z) = 0$  on the surface  $r = a$ , leads to the following

$$E = -\nabla \phi - j\omega A \text{ gives } \nabla \phi = -j\omega A$$

$$\text{and } \nabla^2 A = \frac{-j\beta_0^2}{\omega} \phi \text{ gives } \phi = \frac{1}{\beta_0^2} \nabla^2 A \text{ from which}$$

$$\nabla \phi = \frac{1}{\beta_0^2} \nabla (\nabla^2 A) \text{ Since } A \text{ has only a z-component}$$

on the surface and this is a function of  $z$  alone, we get

$$\frac{d^2 A_z}{dz^2} + \beta_0^2 A_z = 0$$

$$\left( \frac{d^2}{dz^2} + \beta_0^2 \right) A_z(z) = 0 \quad (4.14)$$

on the surface  $\rho = a$

Equation (4.14) has the general solutions

$$A_z(z) = \frac{1}{c} (C_1 \cos \beta_0 z + C_2 \sin \beta_0 z) \quad (4.15)$$

where the symmetry conditions  $I_z(-z) = I_z(z)$ ,  $A_z(-z) = A_z(z)$  are imposed.  $C_1$  and  $C_2$  are arbitrary constants of integration.  $c$  is the velocity of light.

If we use free space Green's function to derive the particular integrals of (4.12) we get for  $A_z$  for a thin cylindrical conductor of length  $2h$  and radius  $a$  with its centre at  $z = 0$  as

$$A_z = \frac{\mu_0}{4\pi} \int_{-h}^h I_z(z') \frac{e^{-j\beta_0 R}}{R} dz' \quad (4.16)$$

where  $\beta_0 = \frac{2\pi}{\lambda_0}$  free space wavelength, and  $R = \sqrt{(Z-Z')^2 + a^2}$ .  
 For a point on the surface  $|z'| = a$ , we combine (4.15) and (4.16) to get the integral equation for the current as

$$\begin{aligned} -\frac{4\pi}{\mu_0} A_Z(Z) &= \int_{-h}^h I_Z(Z') \frac{e^{-j\beta_0 R}}{R} dz' \\ &= \frac{-j4\pi}{\zeta_0} [C_1 \cos \beta_0 Z + C_2 \sin \beta_0 |Z|] \end{aligned} \quad (4.18)$$

where  $\zeta_0 = \sqrt{\mu_0/\epsilon_0} = 120\pi$  ohms.

The one dimensional Lorentz condition is

$$\frac{\partial A_Z}{\partial Z} = \frac{-j\beta_0^2}{\omega} \phi \quad (4.19)$$

From (4.15) and (4.19)

$$\begin{aligned} \phi(Z) &= \frac{j\omega}{\beta_0^2} \left( \frac{\partial A_Z}{\partial Z} \right) \\ &= -C_1 \sin \beta_0 Z + \begin{cases} + C_2 \cos \beta_0 Z & \text{for } Z \geq 0 \\ - C_2 \cos \beta_0 Z & \text{for } Z < 0 \end{cases} \end{aligned} \quad (4.20)$$

By definition the driving voltage of the delta function generator is

$$Z \xrightarrow{Lt} 0 [\phi(Z) - \phi(-Z)] = V_0^e \quad (4.21)$$

Hence  $C_2 = \frac{1}{2} V_0^e$

$$\begin{aligned}
\frac{4\pi}{\mu_0} A_Z(Z) &= \int_{-h}^h I_Z(Z') \frac{e^{-j\beta_0 R}}{R} dZ' \\
&= \frac{-j4\pi}{\xi_0} [C_1 \cos \beta_0 Z + \frac{1}{2} V_0^e \sin \beta_0 |Z|] \\
&\quad (4.22)
\end{aligned}$$

In the above equation (4.22), the constant  $C_1$  can be removed by the following manipulation, consider the following expression

$$\begin{aligned}
4\pi \mu_0^{-1} [A_Z(Z) - A_Z(h)] &= \int_{-h}^h I_Z(Z') K_d(Z, Z') dZ' \\
&= \frac{-j4\pi}{\xi_0} [C_1 \cos \beta_0 Z + \frac{1}{2} V_0^e \sin \beta_0 |Z| + U] \\
&\quad (4.23)
\end{aligned}$$

which is obtained from (4.22) by subtracting  $4\pi \mu_0^{-1} A_Z(h)$  from both sides.

$$U = \frac{-j\xi_0}{4\pi} \int_{-h}^h I_Z(Z') K(h, Z') dZ' \quad (4.24)$$

$$\text{and } K_d(Z, Z') = K(Z, Z') - K(h, Z') \quad (4.25)$$

The constant  $C_1$  can now be expressed in terms of  $U$  and  $V_0^e$  by setting  $Z=h$ . Since the left side of (4.23) then vanishes the right side can be solved for  $C_1$  to give

$$C_1 = \frac{-\left(\frac{1}{2} V_0^e \sin \beta_0 h + U\right)}{\cos \beta_0 h} \quad (4.26)$$



If this value of  $C_1$  is substituted in to (4.23) we get

$$\int_{-h}^h I_Z(Z') K_d(Z, Z') dZ' = \frac{j4\pi}{\cos \beta_0 h} \left[ \frac{1}{2} V_0 e^{\sin \beta_0 (h-|Z|)} + U(\cos \beta_0 Z - \cos \beta_0 h) \right] \quad (4.27)$$

This is an exact expression and does not involve any approximation.

#### 4.3 Use of Approximations

The current  $I_Z(Z)$  vanishes at the ends  $Z = \pm h$  and is continuous through the generator at  $Z=0$ , and satisfies the symmetry condition  $I_Z(-Z) = I_Z(Z)$ . The Kernel in (4.22) is

$$K(Z, Z') = \frac{e^{-j\beta_0 R}}{R}, \quad R = \sqrt{(Z-Z')^2 + a^2} \quad (4.28)$$

Separating into real and imaginary parts

$$K_R(Z, Z') = \frac{\cos \beta_0 R}{R}, \quad K_I(Z, Z') = \frac{\sin \beta_0 R}{R} \quad (4.29)$$

The dimensionless quantities  $K_R(Z, Z')/\beta_0$  and  $K_I(Z, Z')/\beta_0$  are shown graphically in Fig. 4.2 as functions of  $\beta_0 |Z-Z'|$ .  $K_R(Z, Z')/\beta_0$  has a sharp high peak at  $Z=Z'$ , Its magnitude  $(1/\beta_0 a)$  is very large compared with 1 since it has been assumed that  $\beta_0 a \ll 1$

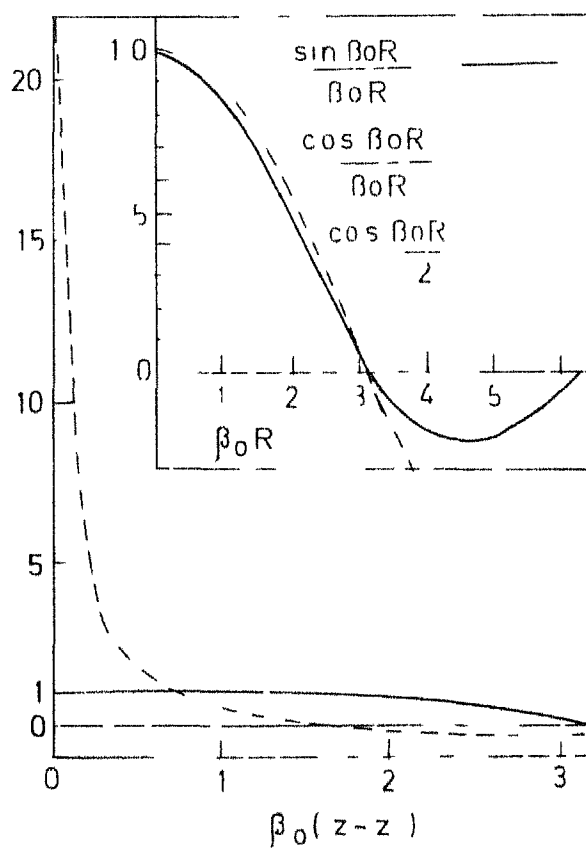


FIG 4 2 THE FUNCTIONS  $\frac{\sin \beta_0 R}{\beta_0 R}$ ,  $\frac{\cos \beta_0 R}{\beta_0 R}$  and  $\cos \frac{\beta_0 R}{2}$

On the other hand  $K_I (Z, Z')/\beta_o$  varies only slowly with  $\beta_o |Z - Z'|$  and never exceeds the value 1. Also  $(\sin \beta_o R/\beta_o R)$  is very well approximated by  $\cos (\beta_o R/2)$  in the range  $0 \leq \beta_o |Z - Z'| \leq \pi$ . The value of  $\cos (\beta_o R/2)$  is hardly affected if the small quantity  $\beta_o a$  is neglected and  $\beta_o R$  is approximated by  $\beta_o |Z - Z'|$ .

Consider now the real and imaginary parts of the integral  $\int_{-h}^h I_Z(Z') \frac{e^{-j\beta_o R}}{R} dZ' = P$  (say)

$$P = P_R + jP_I \quad (4.30)$$

$$\text{Then } P_R(h, Z) = \int_{-h}^h I_Z(Z') \frac{\cos \beta_o R}{R} dZ'$$

$$= \psi_I (Z) I(Z) = \psi_I I(Z) \quad (4.31)$$

$$P_I (h, Z) = - \int_{-h}^h I_Z(Z') \frac{\sin \beta_o R}{R} dZ'$$

$$= - \beta_o \int_{-h}^h I_Z(Z') \cos \frac{1}{2} \beta_o (Z - Z') dZ' \quad (4.32)$$

The reasoning for (4.31) is as follows. Since the Kernel is quite small except at and very near  $Z' = Z$ , where it rises to a very large value, it is clear that the current near  $Z'=Z$  is primarily significant

in determining the value of the integral at  $Z$ . Or simply, the integral is approximately proportional to  $I(Z)$ . The proportionality constant  $\psi_1$  is best determined where  $I_Z(Z)$  is a maximum

This can be further modified by considering that the integral on the left of (4.31) becomes quite small at the ends of the antenna where  $Z = \pm h$ , the RHS vanishes identically at these points since  $I_Z(\pm h) = 0$ . Hence a better approximation of (4.31) is

$$\begin{aligned} P_R(Z) - P_R(h) &= \int_{-h}^h I_Z(Z') [K_R(Z, Z') - K_R(h, Z')] dz' \\ &= \psi_2 I_Z(Z) \end{aligned} \quad (4.33)$$

where  $\psi_2$  is a new constant.

Equation (4.32) can be further simplified

$$P_I(h, Z) = -\beta_0 \int_{-h}^h I_Z(Z') \cos \frac{1}{2} \beta_0 (Z - Z') dz' \quad (4.32)$$

$$\begin{aligned} &= -\beta_0 \int_0^h I_Z(Z') [\cos \frac{1}{2} \beta_0 (Z - Z') + \\ &\quad \cos \frac{1}{2} \beta_0 (Z + Z')] dz' \end{aligned} \quad (4.34)$$

$$\begin{aligned} &= -2 \beta_0 \cos \frac{1}{2} \beta_0 Z \int_0^h I_Z(Z') \cos \frac{1}{2} \beta_0 Z' dz' \\ &\quad (4.35) \end{aligned}$$

For antennas that do not greatly exceed  $\beta_0 h = \pi$  in electrical half length, specifically for  $\beta_0 h \leq 5\pi/4$ ,

$$P_I(h, Z) = P_I(h, 0) \cos \frac{1}{2} \beta_0 Z' \quad (4.36)$$

$$\text{where } P_I(h, 0) = -2 \beta_0 \int_0^h I_Z(Z') \cos \frac{1}{2} \beta_0 Z' dZ'$$

#### 4.4 Derivation of Three - Term Formula

Now in equation (4.27) if we introduce the approximations (4.33) and (4.36), and consider the L.H.S. of (4.27)

$$\text{LHS} = \int_{-h}^h I_Z(Z') K(Z, Z') dZ' - \int_{-h}^h I_Z(Z') K(h, Z') dZ' \quad (4.37)$$

$$\text{Since } K_d(Z, Z') = K(Z, Z') - K(h, Z')$$

$$\begin{aligned} &\approx [\psi_2 I_Z(Z) - j2 \beta_0 \left( \int_0^h I_Z(Z') \cos \frac{1}{2} \beta_0 Z' dZ' \right) \cos \frac{1}{2} \beta_0 Z] \\ &- [0 - j2 \beta_0 \left( \int_0^h I_Z(Z') \cos \frac{1}{2} \beta_0 Z' dZ' \right) \cos \frac{1}{2} \beta_0 h] \end{aligned} \quad (4.38)$$

$$\begin{aligned} &= \psi_2 I_Z(Z) - 2j\beta_0 \left( \cos \frac{1}{2} \beta_0 Z - \cos \frac{1}{2} \beta_0 h \right) \\ &\quad \int_0^h I_Z(Z') \cos \frac{1}{2} \beta_0 Z' dZ' \end{aligned} \quad (4.39)$$

$$\text{Also } U = \frac{-j\epsilon_0}{4\pi} \int_{-h}^h I_Z(Z') K(h, Z') dZ' \quad (4.40)$$

$$= \frac{-j\epsilon_0}{4\pi} \left[ 0 - j2 \beta_0 \cos \frac{1}{2} \beta_0 h \int_0^h I_Z(Z') \cos \frac{1}{2} \beta_0 Z' dZ' \right] \quad (4.41)$$

$$= \frac{j}{4\pi} \epsilon_0 \left[ j2 \beta_0 \cos \frac{1}{2} \beta_0 h \int_0^h I_Z(Z') \cos \frac{1}{2} \beta_0 Z' dZ' \right] \quad (4.42)$$

Considering the RHS of (4.27)

$$\begin{aligned} \text{RHS} = & \frac{j4\pi}{\epsilon_0 \cos \beta_0 h} \left[ \frac{1}{2} V_0^e \sin \beta_0 (h - |Z|) + \right. \\ & \left. (\cos \beta_0 Z - \cos \beta_0 h) \frac{j\epsilon_0}{4\pi} (j2 \beta_0 \cos \frac{1}{2} \beta_0 h) \int_0^h I_Z(Z') \cos \frac{1}{2} \beta_0 Z' dZ' \right] \quad (4.43) \end{aligned}$$

Now transferring the second term of LHS (4.39) to RHS (4.43) and equating LHS and RHS we get,

$$\begin{aligned} \psi_2 I_Z(Z) = & \frac{j4\pi}{\epsilon_0 \cos \beta_0 h} \frac{1}{2} V_0^e \sin \beta_0 (h - |Z|) \\ & + \left[ \int_0^h I_Z(Z') \cos \frac{1}{2} \beta_0 Z' dZ' \right] \cdot \frac{j4\pi}{\epsilon_0 \cos \beta_0 h} \\ & (\cos \beta_0 Z - \cos \beta_0 h) \frac{j^2 2 \beta_0 \epsilon_0}{4\pi} \cos \frac{1}{2} \beta_0 h + j2 \beta_0 (\cos \frac{1}{2} \beta_0 Z \\ & - \cos \frac{1}{2} \beta_0 h) \quad (4.44) \end{aligned}$$

This can be written as follows

$$I_Z(Z) = A[\sin \beta_o(h - |Z|)] + B[\cos \beta_o Z - \cos \beta_o h] \\ + D[\cos \frac{1}{2} \beta_o Z - \cos \frac{1}{2} \beta_o h] \quad (4.45)$$

where

$$A = \frac{j 2\pi V_o e}{\epsilon_o \cos \beta_o h \Psi_2} \quad (4.46)$$

$$B = \frac{-j 2 \beta_o}{\Psi_2} \frac{\cos \frac{1}{2} \beta_o h}{\cos \beta_o h} \int_0^h I_Z(Z') \cos \frac{1}{2} \beta_o Z' dZ' \quad (4.47)$$

and

$$D = \frac{j 2 \beta_o}{\Psi_2} \int_0^h I_Z(Z') \cos \frac{1}{2} \beta_o Z' dZ' \quad (4.48)$$

Thus we have got a three term approximation for current.

The above formulation holds good for the single thin cylindrical conductor case. This theory can be extended to two conductors (see Appendix II) and by induction <sup>to</sup> the general case of N thin cylindrical conductors arranged along the Z axis. Yagi antenna is a special case of this array in which N-1 conductors are parasites and only one element is driven. The solution of this array we will see in the next section.

#### 4.4 Application of Three term Theory to Yagi array

On the basis of the three term approximation the current in the single driven element has the form

$$I_{Z_2}(Z_2) = A_2 M_{0Z_2} + B_2 F_{0Z_2} + D_2 H_{0Z_2} \quad (4.49a)$$

The currents in the parasitic elements are

$$I_{Z_1}(Z_1) = B_1 F_{0Z_1} + D_1 H_{0Z_1} \quad 1 = 1, 3, 4 \quad N \quad (4.49b)$$

where

$$\begin{aligned} M_{0ZK} &= \sin \beta_0 (h_K - |Z_K|) \\ F_{0ZK} &= \cos \beta_0 Z_K - \cos \beta_0 h_K \\ H_{0ZK} &= \cos \frac{1}{2} \beta_0 Z_K - \cos \frac{1}{2} \beta_0 h_K \end{aligned} \quad (4.50)$$

and  $A_1, B_1$  and  $D_1$  are complex coefficients

$A_2, B_1$  and  $D_1$  must be evaluated in terms of the driving voltage  $V_{02}$ . The integral equation for the driven element is

$$\begin{aligned} A_2 \int_{-h_2}^{h_2} M_{0Z'2} K_{21d}(Z_2, Z'_1) dZ'_1 + \sum_{i=1}^N \int_{-h_1}^{h_1} B_1 F_{0Z'_1} K_{21d}(Z_2, Z'_1) dZ'_1 + \sum_{i=1}^N \int_{-h_1}^{h_1} D_1 H_{0Z'_1} K_{21d}(Z_2, Z'_1) dZ'_1 = \frac{14\pi}{\cos \beta_0 h_2} \\ \left[ \frac{1}{2} V_{02} M_{0Z_2} + U_2 F_{0Z_2} \right] \end{aligned} \quad (4.51)$$



Here

$$\begin{aligned}
 K_{K1d}(Z_K, Z'_1) &= K_{K1}(Z_K, Z'_1) - K_{K1}(h_K, Z'_1) \\
 &= \frac{e^{-j\beta_0 R_{K1}}}{R_{K1}} - \frac{e^{-j\beta_0 R_{K1h}}}{R_{K1h}} \quad (4.52)
 \end{aligned}$$

where

$$R_{K1} = \sqrt{(Z_K - Z'_1)^2 + b_{K1}^2}, \quad R_{K1h} = \sqrt{(h_K - Z'_1)^2 + b_{K1}^2} \quad (4.53)$$

and

$$U_K = \frac{-j\beta_0}{4\pi} \sum_{i=1}^N \int_{-h_K}^{h_K} I_{Z1}(Z'_1) K_{K1}(h_K, Z'_1) dZ'_1 \quad (4.54)$$

$$\text{and } \beta_0 = 120\pi$$

The integral equations for the remaining  $(N-1)$  parasitic elements are

$$\begin{aligned}
 A_2 \int_{-h_2}^{h_2} M_{0Z'2} K_{K2d}(Z_K, Z'_2) dZ'_2 \\
 + \sum_{i=1}^N B_i \int_{-h_K}^{h_K} F_{0Z1i} K_{K1d}(Z_K, Z'_1) dZ'_1 \\
 + \sum_{i=1}^N D_i \int_{-h_K}^{h_K} H_{0Z1i} K_{K1d}(Z_K, Z'_1) dZ'_1 \\
 = \frac{14\pi}{-j\beta_0 \cos \beta_0 h_K} U_K F_{0ZK} \quad K=1, 3, \dots, N
 \end{aligned}$$

$$(4.55)$$

In order to obtain approximate solutions of the  $N$  simultaneous integral equations, use may be made of the properties of the real and imaginary parts of the Kernel. That is

$$\int_{-h_K}^{h_K} G_{OZ,K} L_{KKdR} (Z_K, Z'_K) dZ'_K \sim G_{OZK} \quad (4.56)$$

where  $G_{OZ,K}$  stands for  $M_{OZ,K}$ ,  $F_{OZ,K}$  or  $H_{OZ,K}$  and  $L_{KKdR} (Z_K, Z'_K)$  is the real part of the Kernel.

and

$$\int_{-h_K}^{h_K} G_{OZ,K} K_{KKdI} (Z_K, Z'_K) dZ'_K \sim H_{OZK} \quad (4.57)$$

For any distribution  $G_{OZK}$  Hence

$$\begin{aligned} W_{KKV} (Z_K) &\triangleq \int_{-h_K}^{h_K} M_{OZ,K} K_{KKd} (Z_K, Z'_K) dZ'_K \\ &= \psi_{KKdV}^m M_{OZK} + \psi_{KKdV}^h H_{OZK} \end{aligned} \quad (5.58)$$

$$\begin{aligned} W_{KKU} (Z_K) &\triangleq \int_{-h_K}^{h_K} F_{OZ,K} K_{KKd} (Z_K, Z'_K) dZ'_K \\ &= \psi_{KKdU}^f F_{OZK} + \psi_{KKdU}^h H_{OZK} \end{aligned} \quad (4.59)$$

$$\begin{aligned}
 W_{KKD}(Z_K) &\triangleq \int_{-h_k}^{h_k} H_{oZ'K} K_{KdD}(Z_K, Z'_K) |Z'_K| \\
 &= \psi_{KKdD}^f F_{oZK} + \psi_{KKdD}^h H_{oZK}
 \end{aligned} \quad (4.60)$$

where  $\triangleq$  stands for "equal to by definition"

The term  $\psi_{KKdD}^f F_{oZK}$  is added in order to provide greater flexibility and symmetry when  $1 \neq k$  and  $\beta_o b \geq 1$ , it has been shown (Appendix II)

$$\int_{-h_1}^{h_1} G_{oZ'1} K_{KdR}(Z_K, Z'_1) dZ'_1 \sim F_{oZK} \quad (4.61)$$

$$\int_{-h_1}^{h_1} G_{oZ'1} K_{KdI}(Z_K, Z'_1) dZ'_1 \sim H_{oZK} \quad (4.62)$$

Therefore

$$W_{K1V}(Z_K) = \psi_{K1dV}^f F_{oZK} + \psi_{K1dV}^h H_{oZK} \quad (4.63)$$

$$W_{K1U}(Z_K) = \psi_{K1dU}^f F_{oZK} + \psi_{K1dU}^h H_{oZK} \quad (4.64)$$

$$W_{K1D}(Z_K) = \psi_{K1dD}^f F_{oZK} + \psi_{K1dD}^h H_{oZK} \quad (4.65)$$

so we can write from (4.58 - 4.60) and (4.63-4.65) and (4.51)

$$\begin{aligned}
& A_2 [\psi_{22dV}^m M_{oZ2} + \psi_{22dV}^h H_{oZ2}] \\
& + \sum_{i=1}^N B_i [\psi_{21dU}^f F_{oZ2} + \psi_{21dU}^h H_{oZ2}] \\
& + \sum_{i=1}^N D_i [\psi_{21dD}^f F_{oZ2} + \psi_{21dD}^h H_{oZ2}] \\
& = \frac{14\pi}{\sum_o \cos \beta_o h_2} \left[ \frac{1}{2} V_{o2} M_{oZ2} + U_{o2} F_{oZ2} \right] \quad (4.66)
\end{aligned}$$

From (4.55), the (N-1) equations are

$$\begin{aligned}
& A_2 [\psi_{K2dV}^f F_{oZK} + \psi_{K2dV}^h H_{oZK}] \\
& + \sum_{i=1}^N B_i [\psi_{K1dU}^f F_{oZK} + \psi_{K1dU}^h H_{oZK}] \\
& + \sum_{i=1}^N D_i [\psi_{K1dD}^f F_{oZK} + \psi_{K1dD}^h H_{oZK}] \\
& = \frac{14\pi}{\sum_o \cos \beta_o h_K} U_K F_{oZK} \quad K=1, 3, 4, \dots, N \quad (4.67)
\end{aligned}$$

These equations will be satisfied if the coefficient of each of the three distribution functions is individually required to vanish i.e. in (4.66)

$$A_2 = \frac{j 2\pi V_{o2}}{\sum_o \psi_{22dV}^m \cos \beta_o h_2} \quad (4.68)$$

$$\sum_{i=1}^N [B_i \psi_{21dU}^f + D_i \psi_{21dD}^f] \cos \beta_o h_2 \frac{-j 4\pi U_2}{\sum_o} = 0 \quad (4.69)$$

$$A_2 \psi_{22dV}^h + \sum_{i=1}^N [B_i \psi_{21dU}^h + D_i \psi_{21dD}^h] = 0 \quad (4.70)$$

Similarly in (4.67)

$$\left\{ A_2 \psi_{K2dV}^f + \sum_{i=1}^N [B_i \psi_{K1dU}^f + D_i \psi_{K1dD}^f] \right\} \cos \beta_0 h_K - \frac{j4\pi}{\epsilon_0} U_K = 0 \quad (4.71)$$

$$A_2 \psi_{K2dV}^h + \sum_{i=1}^N [B_i \psi_{K1dU}^h + D_i \psi_{K1dD}^h] = 0 \quad (4.72)$$

Defining Kronecker  $\delta$  as

$$\delta_{iK} = \begin{cases} 0 & i \neq K \\ 1 & i = K \end{cases} \quad (4.73)$$

we can combine (4.69, 4.70, 4.71 and 4.72)

The  $2N$  equations are

$$A_2 (1 - \delta_{K2}) \psi_{K2dV}^f + \sum_{i=1}^N [B_i \psi_{K1dU}^f + D_i \psi_{K1dD}^f] \cos \beta_0 h_K - \frac{j4\pi U_K}{\epsilon_0} = 0 \quad (4.74)$$

and

$$A_2 \psi_{K2dV}^h + \sum_{i=1}^N [B_i \psi_{K1dU}^h + D_i \psi_{K1dD}^h] = 0$$

with  $K = 1, 2, 3 \dots N$ . These equations together with (4.68) determine the  $(2N+1)$  constants  $A_2, B_i$  and  $D_i$ ,  $i = 1, 2, 3, \dots N$

Now to evaluate the function  $U_K$ , we define

$$\psi_{K1V}(h_K) = \int_{-h_1}^{h_1} M_{0Z1} K_{K1}(h_K, Z'_1) dZ'_1 \quad (4.75)$$

$$\psi_{K1U}(h_K) = \int_{-h_1}^{h_1} F_{0Z'_1} K_{K1}(h_K, Z'_1) dZ'_1 \quad (4.76)$$

$$\psi_{K1D}(h_K) = \int_{-h_1}^{h_1} H_{0Z'_1} F_{K1}(h_K, Z'_1) dZ'_1 \quad (4.77)$$

where

$$K_{K1}(h_K, Z'_1) = \frac{e^{-j\beta_0 R_{K1h}}}{R_{K1h}},$$

$$R_{K1h} = \sqrt{(h_K - Z'_1)^2 + b_{1K}^2}$$

From (4.54)

$$U_K = \frac{-j\tilde{f}_0}{4\pi} \sum_{i=1}^N [A_i \psi'_{K1V}(h_K) + B_i \psi'_{K1U}(h_K) + D_i \psi'_{K1D}(h_K)] \quad (4.78)$$

Since only element 2 is driven,  $A_1=0$ ,  $i \neq 2$ , so

$$U_K = \frac{-j\tilde{f}_0}{4\pi} \left\{ A_2 \psi_{K2dV}(h_K) + \sum_{i=1}^N [B_i \psi'_{K1U}(h_K) + D_i \psi'_{K1D}(h_K)] \right\} \quad (4.79)$$

The substitution of (4.77) in (4.71) gives

$$A_2 [\psi_{K2V}(h_K) - (1 - \delta_{K2}) \psi_{K2dV}^f \cos \beta_0 h_K] \\ + \sum_{i=1}^N B_i [\psi_{K1U}(h_K) - \psi_{K1dU}^f \cos \beta_0 h_K] \\ + \sum_{i=1}^N D_i [\psi_{K1D}(h_K) - \psi_{K1dD}^f \cos \beta_0 h_K] = 0 \quad (4.80)$$

With  $K = 1, 2, \dots, N$  Let

$$\phi_{K2V} \triangleq \psi_{K2V}(h_K) - (1 - \delta_{K2}) \psi_{K2dV}^f \cos \beta_0 h_K \quad (4.81)$$

$$\phi_{K1U} \triangleq \psi_{K1U}(h_K) - \psi_{K1dU}^f \cos \beta_0 h_K \quad (4.82)$$

$$\phi_{K1D} \triangleq \psi_{K1D}(h_K) - \psi_{K1dD}^f \cos \beta_0 h_K \quad (4.83)$$

with this notation (4.81) with (4.74) gives the following set of  $2N$  equations for determining the  $2N$  coefficients  $B_1$  and  $D_1$  in terms of  $A_2$

$$\sum_{k=1}^N [\phi_{K1U} B_1 + \phi_{K1D} D_1] = - \phi_{K2V} A_2 \quad (4.84)$$

$$\sum_{k=1}^N [\psi_{K1dU}^h B_1 + \psi_{K1dD}^h D_1] = - \psi_{K2dV}^h A_2 \quad (4.85)$$

with  $K = 1, 2, \dots, N$

Here  $\phi_U$ ,  $\phi_D$ ,  $\psi_{dU}^h$  and  $\psi_{dD}^h$  are  $(N \times N)$  matrices and  $\phi_{2V}$ ,  $\psi_{2dV}^h$ ,  $B$  and  $D$  are  $(N \times 1)$  vectors.

The matrix form of (84) and (85) are

$$[\phi_U] \{B\} + [\phi_D] \{D\} = - \{\phi_{2V}\} A_2 \quad (4.86)$$

$$[\psi_{dU}^h] \{B\} + [\psi_{dD}^h] \{D\} = - \{\psi_{2dV}^h\} A_2 \quad (4.87)$$

#### 4.5 Evaluation of $\psi$

Since each integral in (4.58-4.60), (4.63-4.65) and (4.75-4.77) is approximated by a linear combination of two terms with arbitrary coefficients, these can be evaluated by equating both sides in (4.58-4.60) and (4.63-4.65) at two values of  $Z$ . The values chosen are  $Z=0$  and  $Z=h_K/2$  in addition to  $Z=h_K$  where both sides must vanish. We can write

$$\begin{aligned} W_{K1V}(0) &\equiv A_1^{-1} \int_{-h_1}^{h_1} I_{V1}(Z'_1) K_{K1d}(0, Z'_1) dZ'_1 \\ &= \int_{-h_1}^{h_1} M_{0Z'_1} K_{K1d}(0, Z'_1) dZ'_1 \quad (4.88) \end{aligned}$$

$$\begin{aligned} W_{K1V}\left(\frac{h_K}{2}\right) &\equiv A_1^{-1} \int_{-h_1}^{h_1} I_{V1}(Z'_1) K_{K1d}\left(\frac{h_K}{2}, Z'_1\right) dZ'_1 \\ &= \int_{-h_1}^{h_1} M_{0Z'_1} K_{K1d}\left(\frac{h_K}{2}, Z'_1\right) dZ'_1 \quad (4.89) \end{aligned}$$

$$\begin{aligned} W_{K1U}(0) &\equiv B_1^{-1} \int_{-h_1}^{h_1} I_{U1}(Z'_1) K_{K1d}(0, Z'_1) dZ'_1 \\ &= \int_{-h_1}^{h_1} F_{0Z'_1} K_{K1d}(0, Z'_1) dZ'_1 \quad (4.90) \end{aligned}$$

$$\begin{aligned} W_{K1U}\left(\frac{h_K}{2}\right) &\equiv B_1^{-1} \int_{-h_1}^{h_1} I_{U1}(Z'_1) K_{K1d}\left(\frac{h_K}{2}, Z'_1\right) dZ'_1 \\ &= \int_{-h_1}^{h_1} F_{0Z'_1} K_{K1d}\left(\frac{h_K}{2}, Z'_1\right) dZ'_1 \quad (4.91) \end{aligned}$$



$$\begin{aligned}
 W_{K1D}(0) &\equiv D_1^{-1} \int_{-h_1}^{h_1} I_p(z'_1) K_{K1d}(0, z'_1) dz'_1 \\
 &= \int_{-h_1}^{h_1} H_{0Z'_1} K_{K1d}(0, z'_1) dz'_1 \quad (4.92)
 \end{aligned}$$

$$\begin{aligned}
 W_{K1D}\left(\frac{h_K}{2}\right) &\equiv D_1^{-1} \int_{-h_1}^{h_1} I_{D_1}(z'_1) K_{K1d}\left(\frac{h_K}{2}, z'_1\right) dz'_1 \\
 &= \int_{-h_1}^{h_1} H_{0Z'_1} K_{K1d}\left(\frac{h_K}{2}, z'_1\right) dz'_1 \quad (4.93)
 \end{aligned}$$

Here  $K = 1, 2, 3$  .N. These integrations can be converted into generalised sine and cosine integral functions

Then a high speed computer can calculate the ' W's.

Once the W's in (4.88- 4 93) have been obtained for all values of  $l$  and  $K$ , the coefficient  $\psi$  may be determined from the equations (4 58 - 61) and (4.63 - 4.65) At  $Z=0$  these becomes

$$\psi_{KKdV}^m \sin \beta_0 h_K + \psi_{KKdV}^p [1 - \cos(\beta_0 h_K/2)] = W_{KKV}(0) \quad (4.94)$$

$$\psi_{K1dV}^f (1 - \cos \beta_0 h_K) + \psi_{K1dV}^h [1 - \cos(\frac{\beta_0 h_K}{2})] = W_{K1V}(0) \quad l \neq K \quad (4.95)$$

$$\psi_{K1dU}^f (1 - \cos \beta_0 h_K) + \psi_{K1dU}^h [1 - \cos(\frac{\beta_0 h_K}{2})] = W_{K1U}(0) \quad (4.96)$$

$$\psi_{K1dD}^f (1 - \cos \beta_0 h_K) + \psi_{K1dD}^h [1 - \cos(\beta_0 h_K/2)] = W_{K1D}(0) \quad (4.97)$$

At  $Z = h_K/2$ , they are

$$\begin{aligned} \psi_{KKdV}^m \sin(\beta_0 h_K/2) + \psi_{KKdV}^h \left[ \cos\left(\frac{\beta_0 h_K}{4}\right) - \cos\left(\frac{\beta_0 h_K}{2}\right) \right] \\ = W_{KKV}\left(\frac{h_K}{2}\right) \end{aligned} \quad (4.98)$$

$$\begin{aligned} \psi_{K1dV}^f \left[ \cos(\beta_0 h_K/2) - \cos \beta_0 h_K \right] + \psi_{K1dV}^h \left[ \cos \frac{\beta_0 h_K}{4} \right. \\ \left. - \cos \frac{\beta_0 h_K}{2} \right] = W_{K1V}\left(\frac{h_K}{2}\right) \quad 1 \neq K \end{aligned} \quad (4.99)$$

$$\begin{aligned} \psi_{K1dU}^f \left[ \cos(\beta_0 h_K/2) - \cos \beta_0 h_K \right] + \psi_{K1dU}^h \left[ \cos \frac{\beta_0 h_K}{4} \right. \\ \left. - \cos \frac{\beta_0 h_K}{2} \right] = W_{K1U}\left(\frac{h_K}{2}\right) \end{aligned} \quad (4.100)$$

$$\begin{aligned} \psi_{K1dD}^f \left[ \cos \beta_0 h_K/2 - \cos \beta_0 h_K \right] + \psi_{K1dD}^h \left[ \cos \frac{\beta_0 h_K}{4} \right. \\ \left. - \cos \frac{\beta_0 h_K}{2} \right] = W_{K1D}\left(\frac{h_K}{2}\right) \end{aligned} \quad (4.101)$$

The solution of these equations for the  $\psi^-$  are obtained directly. They are

$$\begin{aligned} \psi_{KKdV}^m = \Delta_1^{-1} \left\{ W_{KKV}(0) \left[ \cos \frac{\beta_0 h_K}{4} - \cos \frac{\beta_0 h_K}{2} \right] \right. \\ \left. - W_{KKV}\left(\frac{h_K}{2}\right) \left[ 1 - \cos \frac{\beta_0 h_K}{2} \right] \right\} \end{aligned} \quad (4.102)$$

$$\begin{aligned} \psi_{KKdV}^h = \Delta_1^{-1} \left\{ W_{KKV}\left(\frac{h_K}{2}\right) \sin \beta_0 h_K - W_{KKV}(0) \sin \beta_0 h_K/2 \right\} \end{aligned} \quad (4.103)$$

$$\psi_{K1dV}^h = \Delta_2^{-1} \left\{ W_{K1V}\left(\frac{h_K}{2}\right) [1 - \cos \beta_0 h_K] - W_{K1V}(0) \left[ \cos \frac{\beta_0 h_K}{2} - \cos \beta_0 h_K \right] \right\} \quad 1 \neq K \quad (4.104)$$

$$\psi_{K1dV}^f = \Delta_2^{-1} \left\{ W_{K1V}(0) \left[ \cos \frac{\beta_0 h_K}{4} - \cos \frac{\beta_0 h_K}{2} \right] - W_{K1V}\left(\frac{h_K}{2}\right) [1 - \cos \frac{\beta_0 h_K}{2}] \right\} \quad 1 \neq K \quad (4.105)$$

$$\psi_{K1dU}^f = \Delta_2^{-1} \left\{ W_{K1U}(0) \left[ \cos \frac{\beta_0 h}{4} - \cos \frac{\beta_0 h_K}{2} \right] - W_{K1U}(h_{K/2}) [1 - \cos \frac{\beta_0 h_K}{2}] \right\} \quad (4.106)$$

$$\psi_{K1dU}^h = \Delta_2^{-1} \left\{ W_{K1U}\left(\frac{h_K}{2}\right) [1 - \cos \beta_0 h_K] - W_{K1U}(0) \left[ \cos \frac{\beta_0 h_K}{2} - \cos \beta_0 h_K \right] \right\} \quad (4.107)$$

$$\psi_{K1dD}^f = \Delta_2^{-1} \left\{ W_{K1D}(0) \left[ \cos \frac{\beta_0 h_K}{4} - \cos \frac{\beta_0 h_K}{2} \right] - W_{K1D}\left(\frac{h_K}{2}\right) [1 - \cos \frac{\beta_0 h_K}{2}] \right\} \quad (4.108)$$

$$\psi_{K1dD}^h = \Delta_2^{-1} \left\{ W_{K1D}\left(\frac{h_K}{2}\right) [1 - \cos \beta_0 h_K] - W_{K1D}(0) \left[ \cos \frac{\beta_0 h_K}{2} - \cos \beta_0 h_K \right] \right\} \quad (4.109)$$

where

$$\Delta_1 \triangleq \sin \beta_0 h_K [\cos (\beta_0 h_K/4) - \cos (\beta_0 h_K/2)] - \sin (\beta_0 h_K/2) [1 - \cos (\beta_0 h_K/2)] \quad (4.110)$$

and

$$\begin{aligned} \Delta_2 \triangleq & [1 - \cos \beta_0 h_K] \left[ \cos \frac{\beta_0 h_K}{4} - \cos \frac{\beta_0 h_K}{2} \right] \\ & - \left[ \cos \frac{\beta_0 h_K}{2} - \cos \beta_0 h_K \right] \left[ 1 - \cos \frac{\beta_0 h_K}{2} \right] \end{aligned} \quad (4.111)$$

Thus first all the  $\psi$ 's are determined from (4.102 to 4.111). Then the  $\phi$  matrix elements are computed from (4.81 - 4.83). Finally solving equation (4.37~~48~~)

$$\begin{bmatrix} [\phi_U] & [\phi_D] \\ [\psi_{dU}^h] & [\psi_{dD}^h] \end{bmatrix} \begin{Bmatrix} B \\ D \end{Bmatrix} = \begin{Bmatrix} -\phi_{2V} A_2 \\ -\psi_{2dV}^h A_2 \end{Bmatrix} \quad (4.112)$$

$$\begin{Bmatrix} B \\ D \end{Bmatrix} = \begin{bmatrix} [\phi_U] & [\phi_D] \\ [\psi_{dU}^h] & [\psi_{dD}^h] \end{bmatrix}^{-1} \begin{Bmatrix} -\phi_{2V} A_2 \\ -\psi_{2dV}^h A_2 \end{Bmatrix} \quad (4.113)$$

We get  $B_1$ 's and  $D_1$ 's.  $A_2$  was already calculated from (4.68). Substituting all these in (4.49) and (4.50) gives current in all the segments of Yagi-Uda array.

## CHAPTER 5

### COMPUTATIONS FOR PATTERN, GAIN AND IMPEDANCE

#### 5.1 General

Once the current in each segment of every element of the array is found, we can calculate the Input Impedance and Admittance of the Yagi antenna, Radiation field pattern, gain of the antenna and directivity of the antenna using computers

#### 5.2 Input Impedance

The input impedance of the Yagi antenna is measured at the feed points of the driven element i.e. at the center of the 2nd element in the array. The input impedance helps us in designing the receiver circuits

The input impedance calculation in a computer analysis is very simple. As we assume that the excitation is one volt, the reciprocal of the current at the middle of the second element,  $I_{Z_2}$  (21,2) will directly give us the Input admittance. The reciprocal of the Input admittance is the input impedance.

#### 5.3 Pattern Measurement

The far field or radiation field of an antenna is one of its most important characteristics. The field

pattern is actually a three dimensional or space pattern, and its complete description requires field intensity calculations in all directions in space.

A space pattern can be calculated according to the following procedure. Let us keep the antenna at the origin with the  $x_y$  plane horizontal and the  $Z$  axis vertical as in Fig 5.1. Then on an imaginary sphere of large radius with the origin at the centre, patterns of  $\theta$  and  $\phi$  components of the electric field ( $E_\theta$ ,  $E_\phi$ ) are calculated along latitude circles (that is circles of constant latitude or polar angle,  $\theta$ ). These patterns are calculated as a function of the longitude or azimuth angle  $\phi$ . Calculating such patterns at  $5^\circ$  intervals in latitude from  $\theta = 0$  to  $180^\circ$  and  $\phi = 0^\circ$  to  $360^\circ$  completely describes the radiated field.

From King (16) we know that the radiation field for a thin cylindrical conductor of length  $2h$  and radius  $a$  with its centre at  $Z=0$ ,

$$E^\theta = \frac{j \mu_0 I_0 a}{4\pi} \sin \theta \int_{-h}^h I_z(Z') \frac{e^{-j\beta_0 R}}{R} dz' \quad (5.1)$$

where  $R$  is the distance from an arbitrary point on the antenna to the field point and is given in terms of  $r$  and  $Z'$  by the cosine law (Fig 5.2)

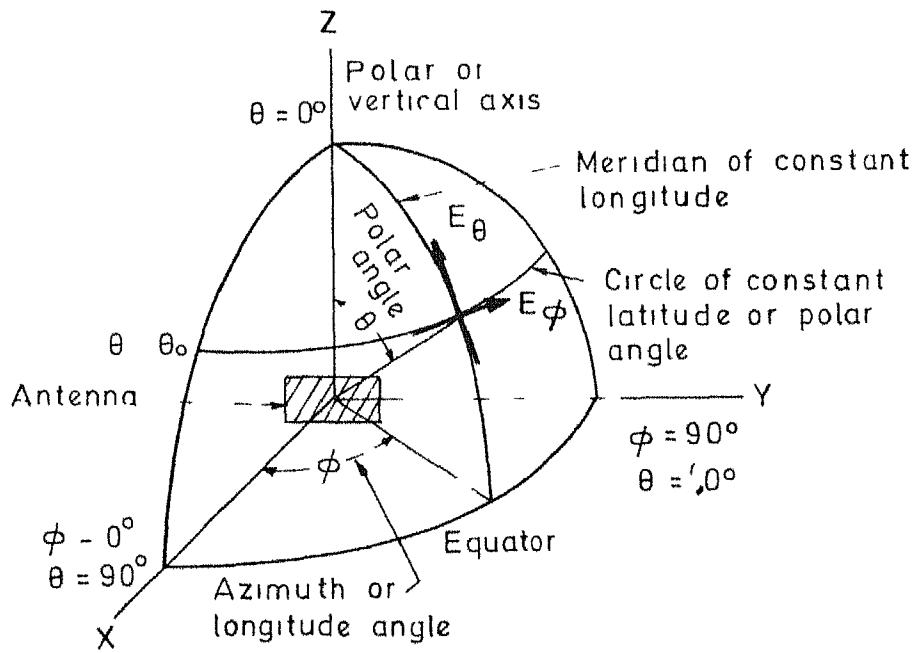


FIG 51 ANTENNA AND COORDINATES FOR PATTERN MEASUREMENTS

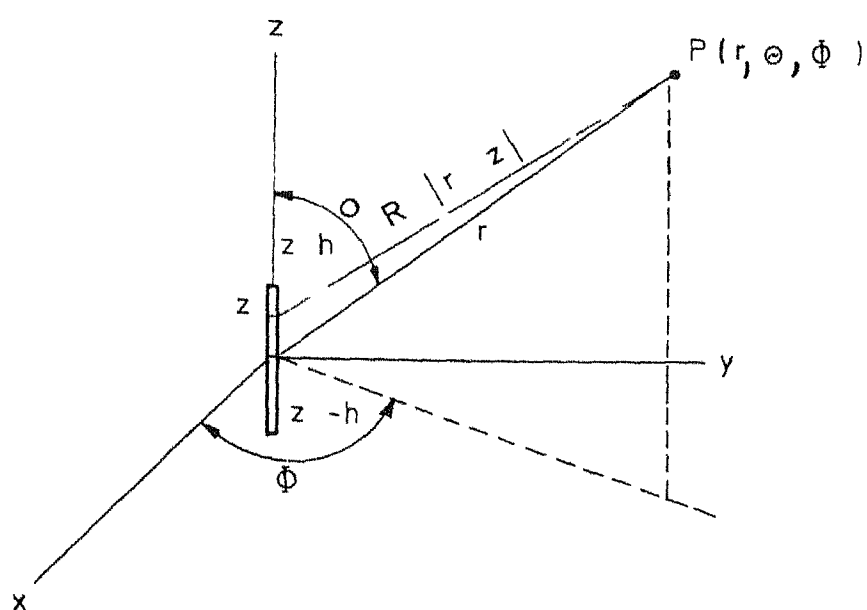


FIG 5 2 COORDINATE SYSTEM FOR CALCULATIONS IN THE FAR ZONE



$$R^2 = r^2 + (Z')^2 - 2 r Z' \cos \theta \quad (5.2)$$

In the radiation zone  $r^2 \gg (Z')^2$ . If the binomial expansion is applied to (5.2) and only the linear term in  $Z'$  is retained, the following approximate form is obtained for  $R$

$$R = r - Z' \cos \theta, \quad (\beta_0 r)^2 \gg 1 \quad (5.3)$$

The phase variation of  $\exp(-j\beta_0 R)/R$  is replaced with the linear phase variation given by (5.3) i.e. by  $\exp(-j\beta_0 R + j\beta_0 Z' \cos \theta)$ . The amplitude  $1/R$  of  $\exp(-j\beta_0 R)/R$  is a slowly varying function of  $Z'$  and is replaced by  $1/r$ , where  $r$  is the distance to the centre of the antenna. Since  $r$  is independent of  $Z'$  all functions of  $r$  may be removed from the integral in 5.1 and the final form for  $E^x$  is

$$E^x = \frac{j\mu_0\omega}{4\pi} \sin \theta \frac{e^{-j\beta_0 r}}{r} \int_{-h}^h I_Z(Z') e^{j\beta_0 Z' \cos \theta} dZ' \quad (5.4)$$

Now to determine the electric field maintained at distant points by the currents in the  $N$  elements of the Yagi Uda array, we find that for

$$\begin{aligned} I_{Z_2}(Z_2) = & A_2 \sin \beta_0 (h_2 - |Z_2|) \\ & + B_2 (\cos \beta_0 Z_2 - \cos \beta_0 h_2) \\ & + D_2 (\cos \frac{1}{2} \beta_0 Z_2 - \cos \frac{1}{2} \beta_0 h_2) \end{aligned} \quad (5.5)$$

and

$$I_{Z_1}(Z_1) = B_1 (\cos \beta_0 Z_1 - \cos \beta_0 h_1) \\ + D_1 (\cos \frac{1}{2} \beta_0 Z_1 - \cos \frac{1}{2} \beta_0 h_1) \\ 1 \neq 2 \quad (5.6)$$

the electromagnetic field is

$$E(R_2, \theta, \phi) = \frac{J_0 \mu_0}{4\pi} \sin \theta \sum_{1=1}^N \frac{e^{-j\beta_0 R_1}}{R_1} \\ \int_{-h_1}^{h_1} I_{Z_1}(Z'_1) e^{j\beta_0 Z'_1 \cos \theta} dZ'_1 \quad (5.7)$$

Referring to Fig 5.3, we make the far-field approximation  $R_1 = R_2 = r_0$  in amplitude. However in phase,

$$R_1 - R_2 = -(1-2)b \sin \theta \cos \phi \quad (5.8)$$

where 1 is the 1th element number and 'b' is the inter-element spacing. As we have defined  $d_1 = -(1-2)b$ , the equation (5.7) becomes

$$E^r(\theta, \phi) = \frac{J_0 \mu_0}{4\pi r_0} \sum_{1=1}^N e^{j\beta_0 d_1 \sin \theta \cos \phi} \\ \int_{-h_1}^{h_1} I_1(Z'_1) e^{j\beta_0 Z'_1 \cos \theta} \sin \theta dZ'_1 \quad (5.9)$$

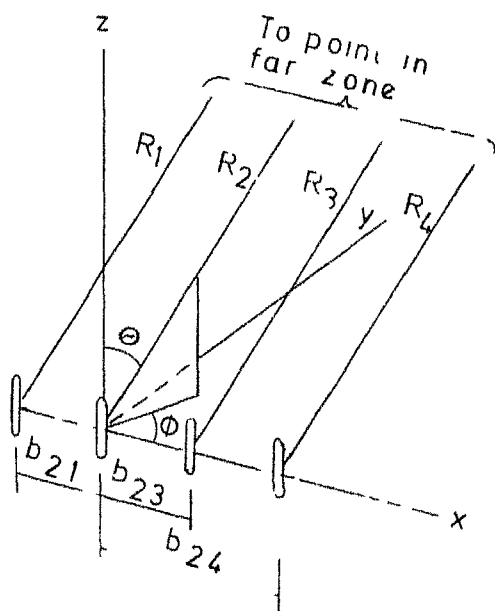


FIG 5 3 COORDINATES FOR 4 ELEMENT ARRAY REFFERENCE  
TO ORIGIN AT CENTRE OF ELEMENT 2

$$b_{21} \quad b_{23} = b_{34} = b$$

Equation (5 9) was used to calculate the E field pattern  $E(\pi/2, \phi)$  gives the Azimuthal or Horizontal pattern

#### 5 4 Gain

The gain of an antenna is defined as

$$\text{Gain} = \frac{\text{Maximum Radiation intensity (test antenna)}}{\text{Maximum Radiation intensity (reference antenna)}} \quad (5 10)$$

It is ideal to consider a reference antenna which radiates uniformly in all directions with gain of unity. But in practice as no isotropic radiator is available, we use a dipole as a reference which has a gain of 1.64 over the isotropic radiator.

We are more interested in Directivity since Yagi antenna is a directive antenna.

$$\text{Directivity} = \frac{\text{Maximum radiation intensity}}{\text{Average radiation intensity}} \quad (5 11)$$

If we take that the antenna radiates a maximum in the direction  $(\theta_0, \phi_0)$

The radiation intensity  $U$  is related to the Poynting vector  $P$  which in turn is related to the Electric field intensity  $E$  (25)

$$P = \frac{1}{2} \frac{E^2}{Z_0} \quad (5 12)$$

where  $Z_0$  is the intrinsic impedance of the free space  
 The radiation intensity is the power per unit solid  
 angle and is equal to  $r^2$  times  $P$  Moreover by multi-  
 plying the numerator and denominator of (5 11) we get

$$\text{Directivity} = \frac{4 \pi |E(\theta_0, \phi_0)|^2}{\text{Total power radiated}} \quad (5 13)$$

If we take that the antenna radiates a maximum in  
 the direction  $(\theta_0, \phi_0)$  The total power radiated

$$= \int_0^{2\pi} d\phi \int_0^\pi |E'(\theta, \phi)|^2 \sin \theta d\theta d\phi \quad (5 14)$$

Hence Directivity is calculated from the radiation  
 pattern and from (5 12) and (5 13).

## 5 5 Conclusion

The theoretical calculation of impedance,  $E$  field  
 pattern and gain are described in this chapter A  
 computer listing appearing in the appendix will indicate  
 the calculation procedure

## CHAPTER 6

### ANTENNA MEASUREMENTS

#### 6.1 General

In the last chapter we saw the theoretical calculation procedures using a computer. In the present chapter the practical measurement set up is explained

#### 6.2 Antenna

As we designed the Yagi antenna for channel IV whose centre frequency we took as 65 MHz, the following are the dimensions of the antenna for a initial set up. Since the wavelength ( $\lambda$ ) is 4.615 meters, the radius of the elements is taken as 1 5 cms, the reflector 1 177 meters, the driven element 1 130 meters and the directors 99 2 cms. The spacing between the reflector and the driven element is 1 154 meters and the other interelement spacings are 1 43 meters

However, in order to check Cheng and Chen's optimization results, the antenna was made with provisions to vary the element spaces as well as the lengths. A locknut arrangement was used to move the elements along the cross boom and concentric tubes were used

to vary the lengths of the elements. The main cross boom length is 8.1 meters. The height of the antenna is approximately 3.5 meters from ground level.

A folded dipole was used for the driven element as this facilitates the use of the 300  $\Omega$  TV cable as feeder. (Folded dipole impedance  $\sim 300\Omega$ ). A balun was used to provide matching between the balanced and unbalanced circuits of the antenna. The Fig 6.1 shows the Balun construction details (29)

For a test transmitter antenna, a folded dipole whose length was also 4.615 meters was constructed. The photoes at the end of the thesis explains the physical set up

Experimental measurements on antennas become difficult on account of the fact that all antenna parameters are affected by reflections from nearby objects. To get over this difficulty, all measurements were made on the roof of the building in an environment relatively free from reflections.

### 6.3 Impedance Measurement

The impedance measurement set up is shown in Fig 6.2. A Hewlet Packard Vector Voltmeter was used to measure directly the reflection coefficient (both

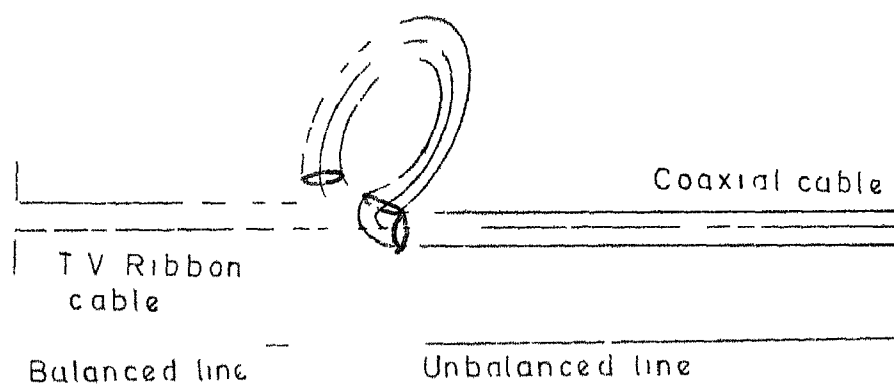


FIG 61 BALUN CONSTRUCTION 4 TO 1 IMPEDENCE TRANSFORMER



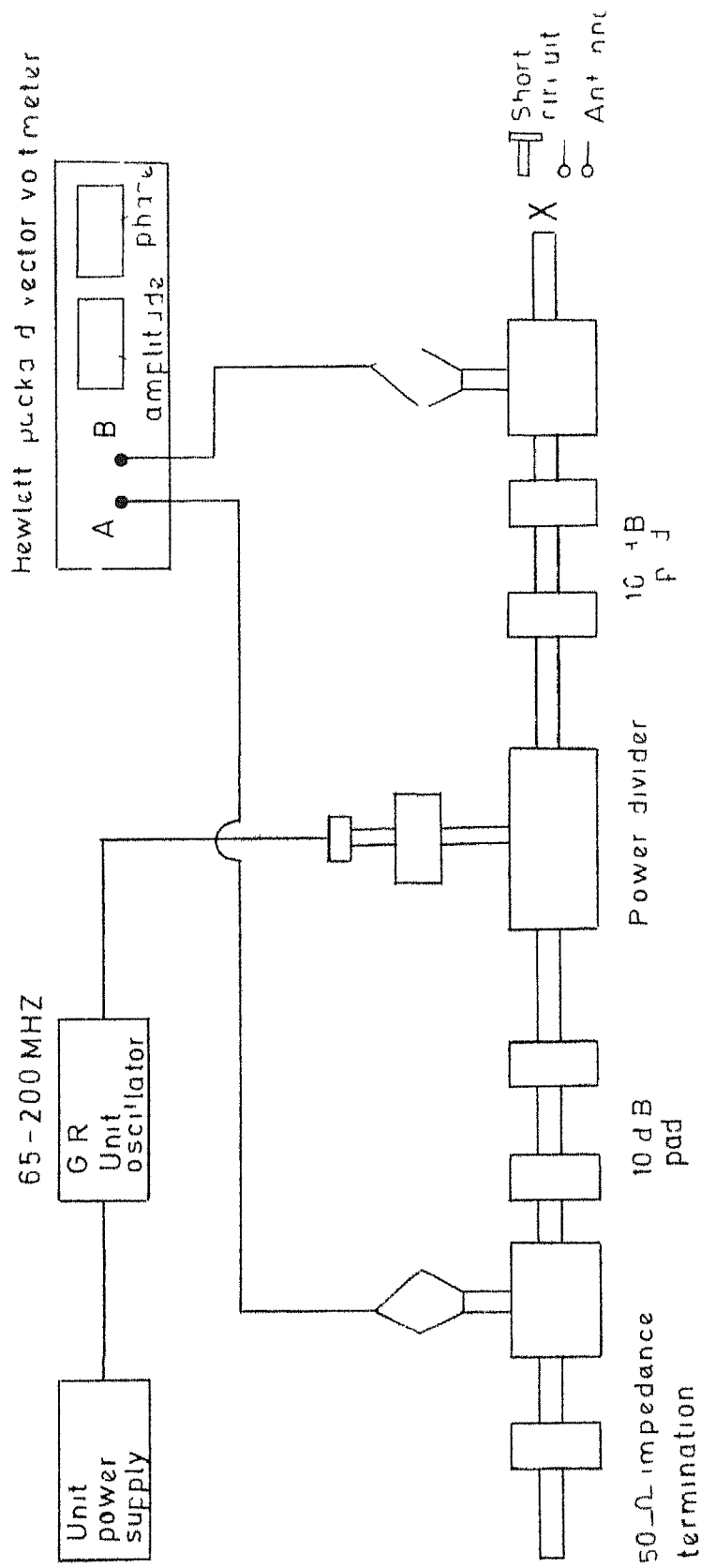


FIG 6 2 IMPEDENCE MEASUREMENT

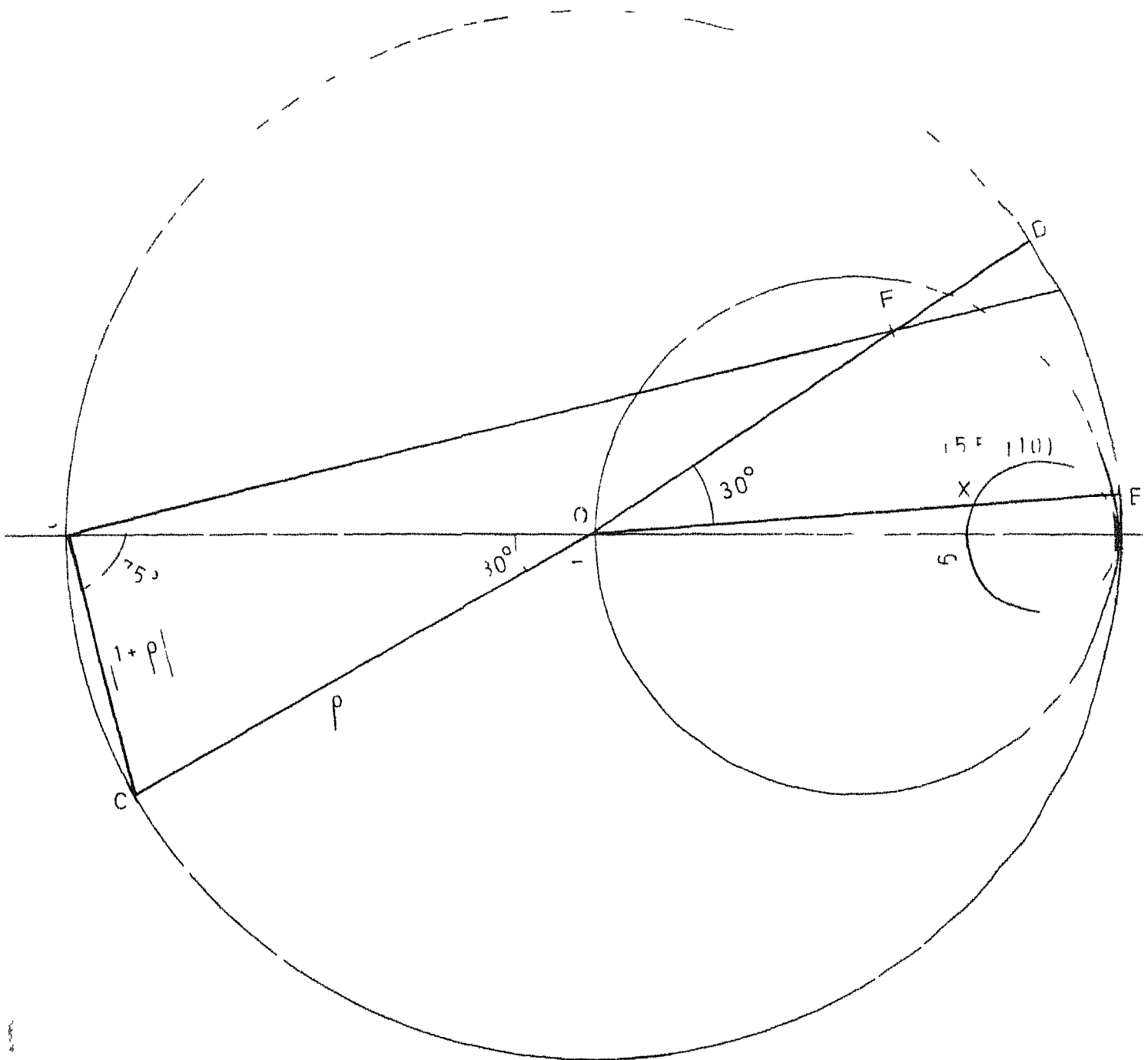


FIG 6 3 IMPEDENCE MEASUREMENT USING SMITH CHART

have to be off set by  $30^\circ$  in the opposite or CW direction, in order to correct for this initial phase off set.

After replacing the short with the antenna,  $B/A$   $1 + j^5$  is now measured to be  $1.62 \angle +14^\circ$ . The point F must then be rotated CW. This angle can be plotted by striking off from point D the distance SC with a pair of dividers to where it intersects the circumference of the chart at E. The magnitude of  $\beta$  of the antenna, OF is then measured off from O along OE. This point X equals 50 ( $5.5 + j 10$ ) or ( $275 + j50$ ) ohms whose magnitude 280 ohms is close to 300 ohms for a folded dipole.

#### 6.4 Pattern Measurement

To measure the far field pattern of the antenna, the distance between the Transmitting and the Receiving antennas must be appropriate. If this distance is too small, then the near field or Fresnel pattern is obtained. The Fresnel pattern is a function of the distance at which it is measured. For accurate far-field measurements the antenna under test should be illuminated with a plane wave front. Since plane wave fronts, are obtainable only at infinite distances, some limits must be specified. A commonly specified criterion is

that the phase difference between the centre and edges of the antenna under test shall be no greater than  $\lambda/16$ . If this is the case, then from Fig. 6.4

$$(R+\delta)^2 = R^2 + \left(\frac{d}{2}\right)^2 \quad (6.1)$$

and

$$R^2 + 2\delta R + \delta^2 = R^2 + \frac{d^2}{4} \quad (6.2)$$

For  $R \gg \delta < d$ ,  $\delta^2$  may be neglected, and

$$R \approx \frac{d^2}{8\delta} \quad (6.3)$$

$$\text{For } \delta = \lambda/16, R \gg 2 d^2/\lambda \quad (6.4)$$

The receiving antenna aperture is approximately  $2\lambda$  and hence  $R \gg 8\lambda$ . We kept a distance of approximately  $10\lambda$  between the Transmitter and the Receiver (Fig. 6.5). Moreover in order to avoid ground reflections, the transmitter and receiver antennas were mounted on two sections of the terrace of Western Laboratory of IIT Kanpur with a valley between the two sections.

The Yagi antenna is mounted on a Mast of height about 10 feet. At the base of the mast, an outer tube of a larger diameter is embedded in a square concrete structure. A circular disc with degrees marked on it for every  $10^\circ$  is attached to this outer tube. The inner tube (mast) <sup>has</sup> a pointer attached to it

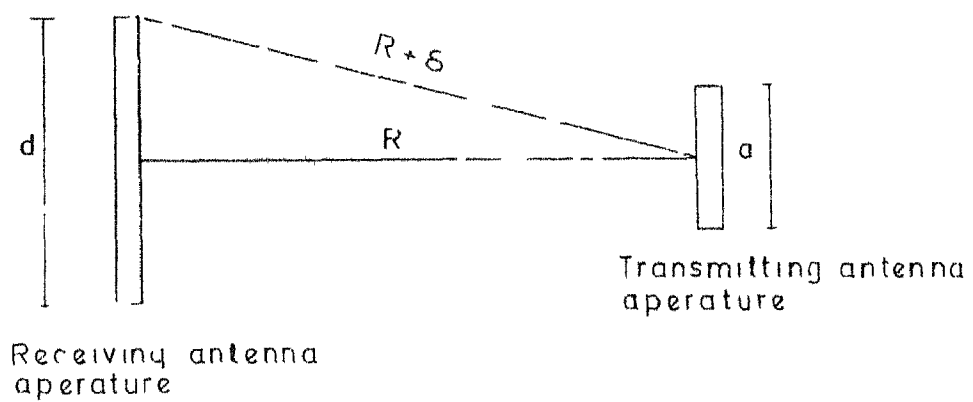
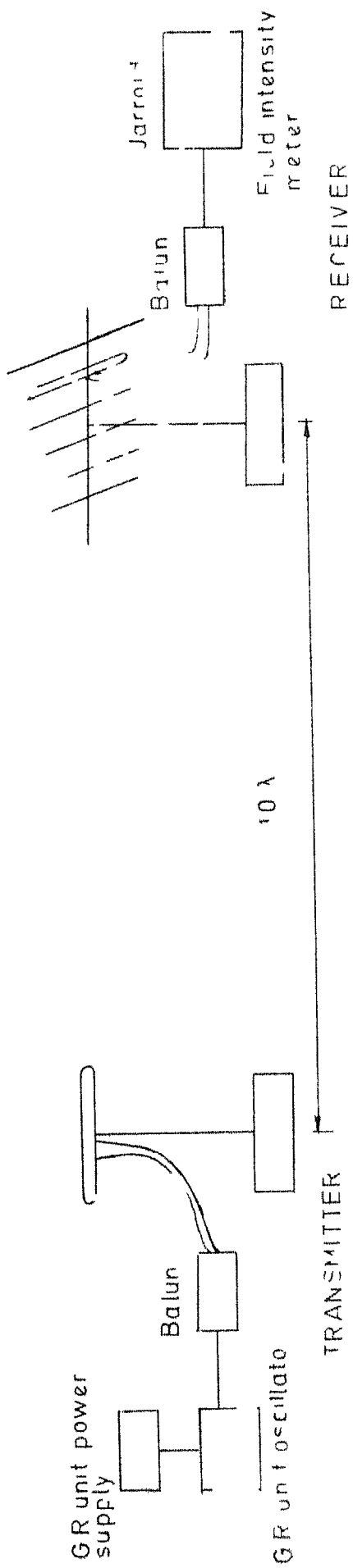


FIG 6 4 PHASE DIFFERENCE BETWEEN CENTER AND  
EDGE OF RECEIVING APERTURE



so that when the mast and hence the antenna is rotated, the pointer indicates the angular movement accurately. The arrangements are shown in Figs 6.8, 6.6 and 6.7.

The transmitter was adjusted for maximum output power. The antenna pointer was fixed at a reference angle  $\phi = 0^\circ$ . The reading on the Jarrolds Field intensity meter was noted.

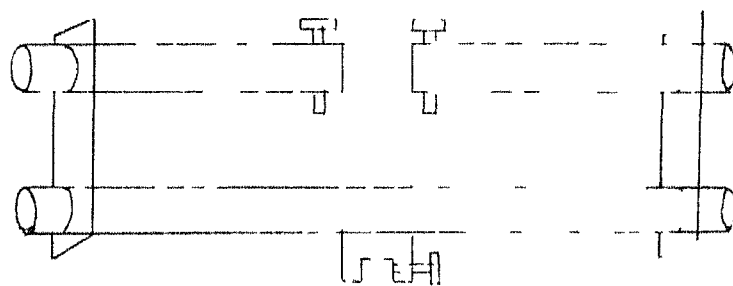
Field intensity for every  $10^\circ$  was noted and plotted in a circular graph, for an initial arrangement of Cheng and Chen. The final arrangement was then made for the elements and spacings of the array and the measurement and plotting was repeated. Normalized values were used in the circular plot.

#### 6.5 Gain Measurement

The gain measurement was done by the substitution method. First a folded dipole was kept in the place of Yagi array and adjustments were made between the transmitter and receiver such that the receiver output is maximum. Then the dipole is replaced by the Yagi antenna. Again maximum field strength is noted. Then,

$$\text{Directivity} = \frac{\text{output of Receiver with Yagi}}{\text{output of Receiver with Dipole}}$$

(6.5)



Lock nut

FIG 6 6 FOLDED DIPOLE



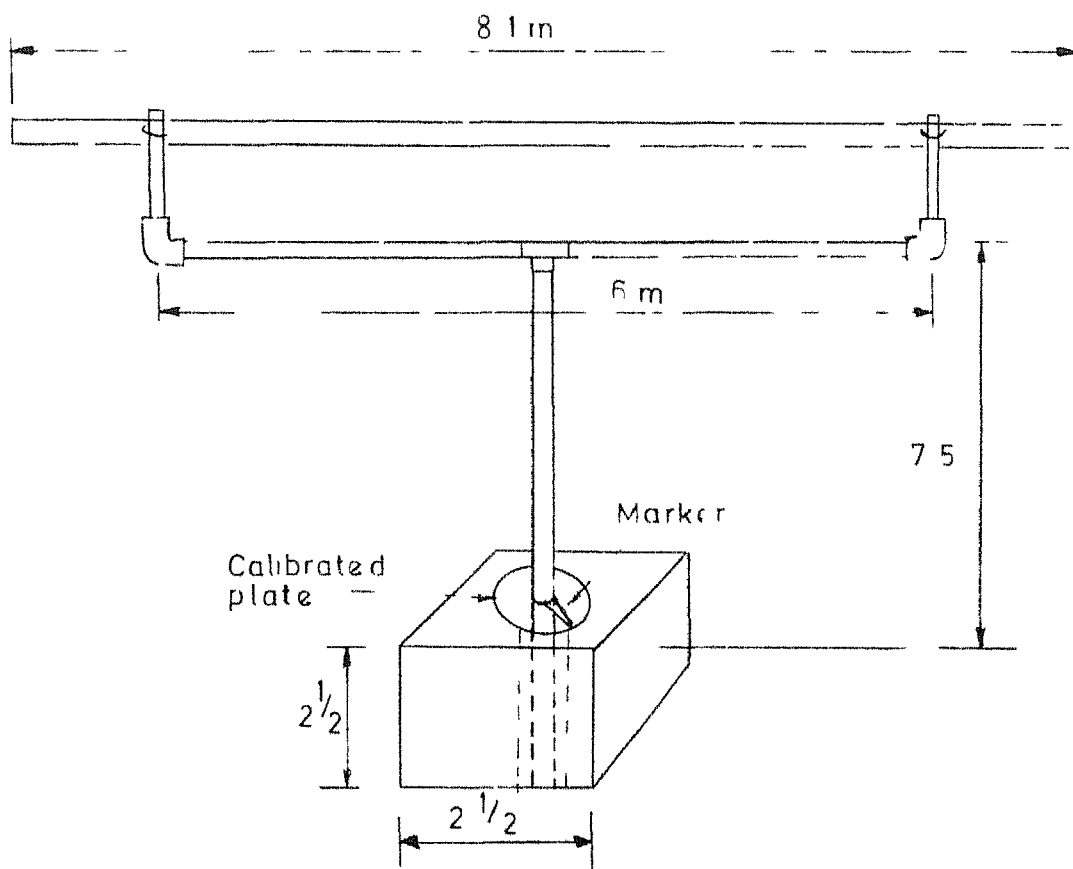
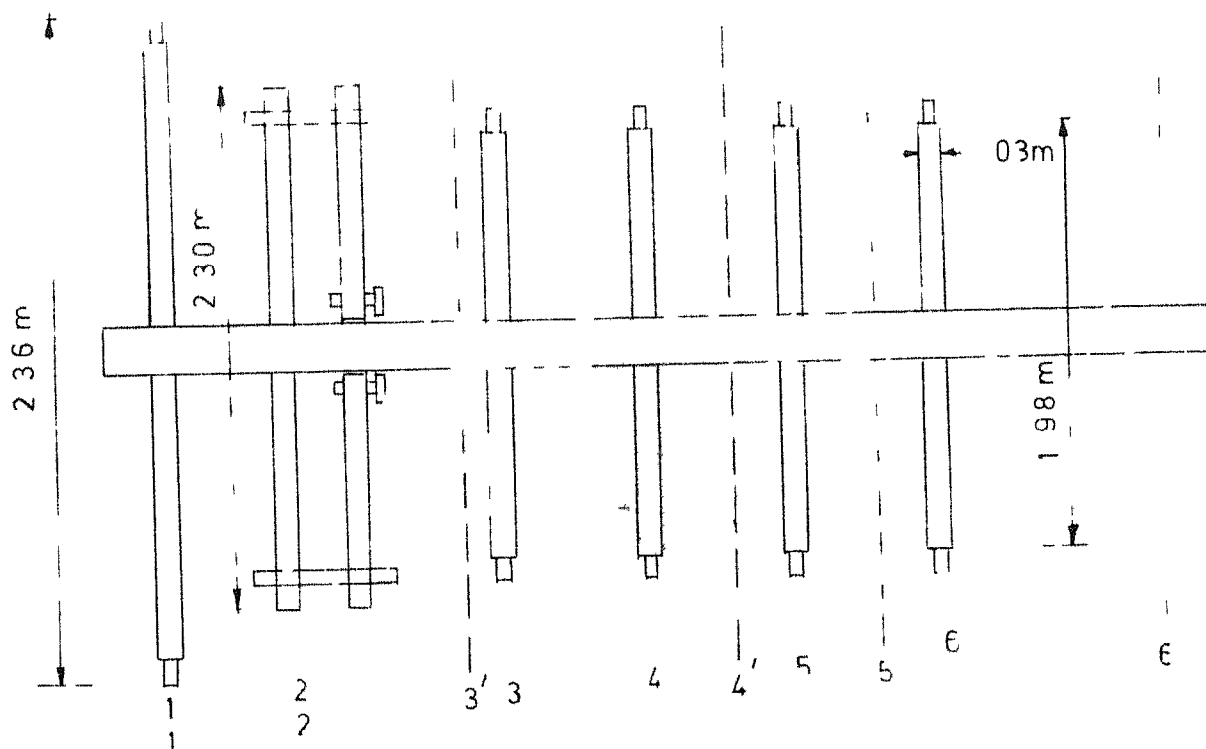


FIG 6 7 MAST



1 - 6 Initial array pacing

1' 6 Optimum array spacing

FIG 6 8 PHYSICAL LAYOUT OF THE YAGI ANTENNA

The experiment was repeated with Kanpur T.V. station as a transmitter. Also gain for optimized array was measured. The results of this chapter appears in the next chapter.

## CHAPTER 7

### RESULTS AND DISCUSSIONS

#### 7.1 General

There are three types of results which are available to us. King has published some results in his book 'Arrays of Cylindrical dipole' and Cheng and Chen have given optimization results in their Technical Report. The author of this thesis has formulated a computer program which appears in Appendix III which computes input impedance, current distribution in the elements, Directivity and gain and Electric field pattern. The computer results are compared with King and Cheng and Chen results. The author has also constructed a Yagi antenna to the specifications of Cheng and Chen to verify experimentally their claim of increased gain with optimum element spacing and length. The experimental and theoretical results agree to a large extent.

#### 7.2 Computed results vs Published Results

King has given the current distribution in two full wave dipoles, one reflector and one driven element. Table 7.1 shows the correspondence between the published  $A_2$ ,  $B_1$  and  $D_1$  values (the complex coefficients of the

Table 7 1

Item	King's Results	Computed Results
A <sub>2</sub>	-0 249E - 04 -j0 318E - 02	-0.250E - 04 -j 319E - 02
B <sub>1</sub>	0 708E - 04 -j0 493E- 03	0.752E- 04 -j0 473E - 03
B <sub>2</sub>	0.183E - 03 +j0.441E-03	0 188E - 03 +j0 437E- 03
D <sub>1</sub>	0.221E - 03 +j0.456E-03	0.217E - 03 +j0.441E- 03
D <sub>2</sub>	0 439E - 03 +j0.627E- 03	0 445E - 03 +j0 628E -03

Table 7.2

Item	Gain results by Cheng and Chen(wr to isotr- opic radiator)		Computed Results
	as ratio	as decible	
1 Initial array	12.372	10.92 dB	12.2, 10.87 dB
2. Length perturbed array	16.42	12.15 dB	16.08, 12.06 dB
3 Spacing perturbed array	19.16	12.82 dBB	19 0, 12 79 dB
4. Optimized array	21 9	13 4 dB	21 8 , 13.38 dB

3 term currents distribution) and the computed values for a two element array

Table 7 2 compares the gain results published by Cheng and Chen with the computed values Their claim that optimization of length and spacing increases gain is thus verified The corresponding impedance values also show that the program is reliable Fig. 7.1 shows the current distribution in various elements of the array. The difference between the computed pattern and Cheng's pattern published is negligible .

### 7 3 Experimental Results vs Computed Results

#### 7 3 1 Radiation Pattern

Here the experimental set up described in Chapter 6 was used to see the optimization results. Fig 7.2 gives a polar graph representation of the pattern which also compares the experimental and theoretical values The experimental pattern shows lower side lobes and a higher back lobe than the theoretical curve This may be due to the fact that in theory the driven element is a single dipole but in the experiment, the driven element is a folded dipole Also the diameter of the elements were not exactly that of the theoretical value Still we can see that the peaks and troughs of the patterns coincide.

x Real  
o Imaginary

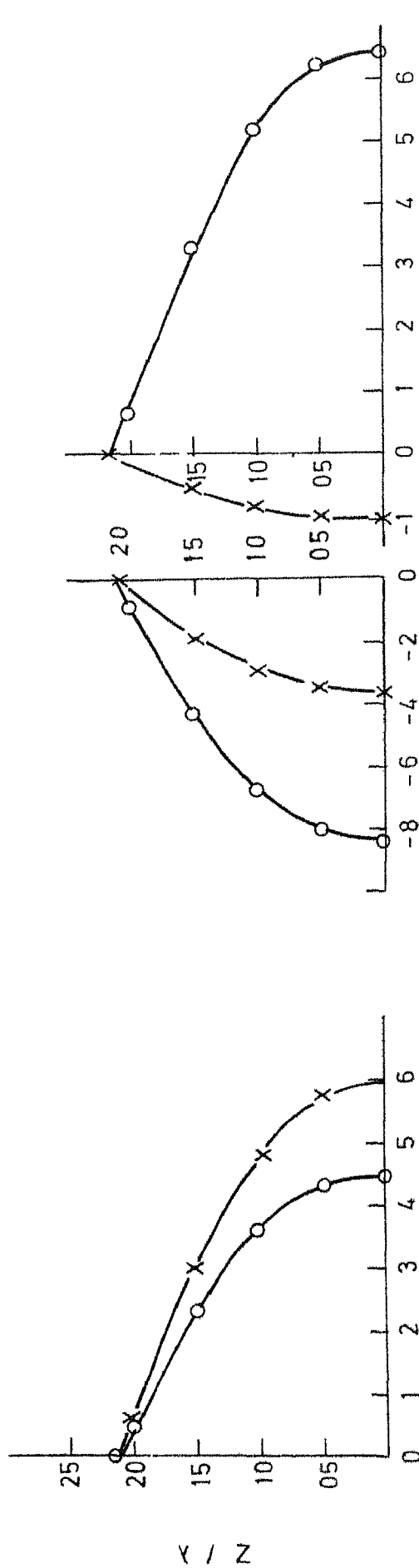
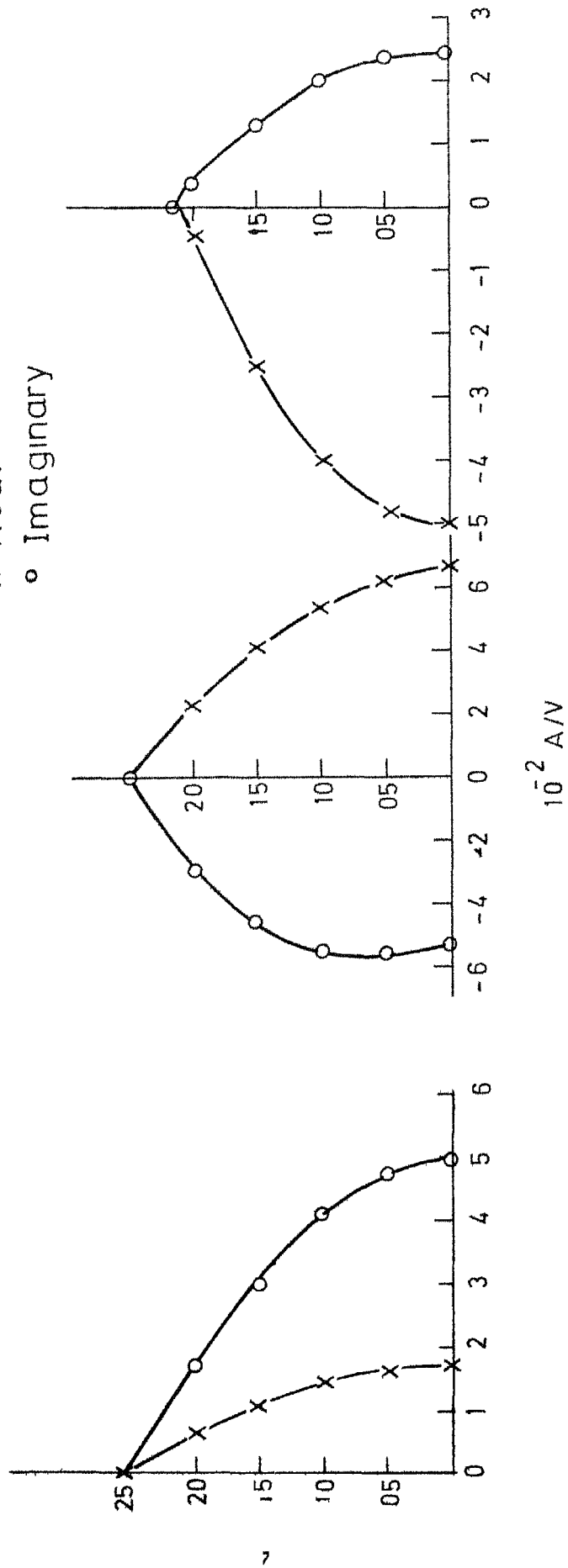


FIG 71 CURRENT DISTRIBUTION IN YAGI ANTENNA WITH INITIAL ARRANGEMENT

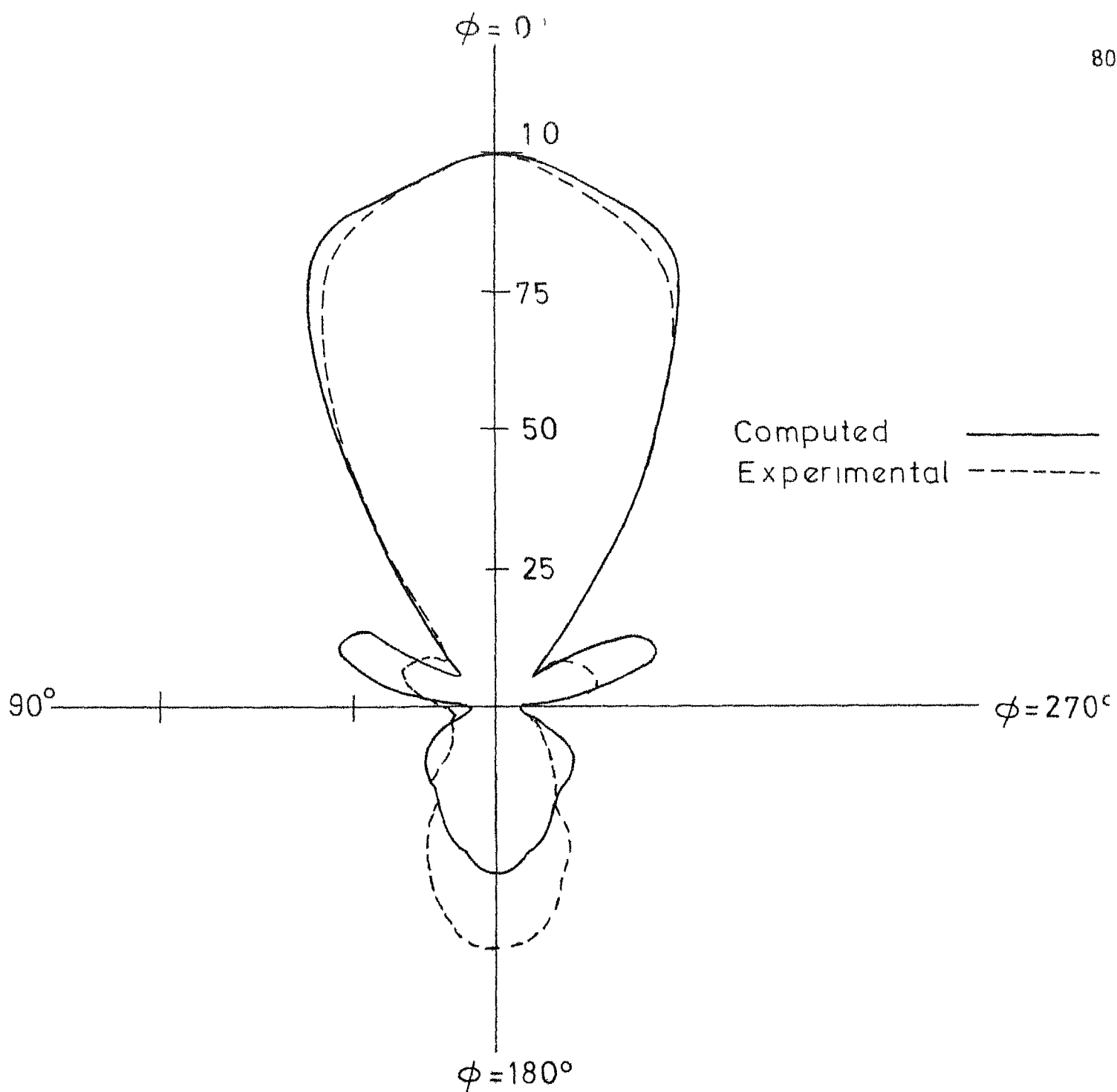


FIG 7 2 E-FIELD PATTERN OF YAGI-UDA ANTENNA



### 7.3 2 Input Impedance and Gain

The impedance measurement values are compared in Table 7 3. Gain values are also compared in the same table. Fig 7.3 compares the initial, space perturbed and final patterns.

Apart from these experiments which were based on the published results, computer analysis was carried on to find the Bandwidth of the antenna. The computed values are shown in Table 7.4 and plotted in Fig. 7.4.

It is worthwhile to evaluate the performance of a given Yagi antenna over several TV channels. This is particularly true in situations like the Lucknow TV broadcasting on Channel IV (centre frequency 65 MHz) and a relay station at Akrapur relaying, the same programme on Channel V (centre frequency 174 MHz ) and many times the same antenna is used for both. For this purpose, the gain of the Channel IV antenna for higher frequencies was also computed and this is shown in Table 7.5.

The pattern for Kanpur Television (Channel V) on a Channel IV antenna was found to have an almost nondirectional pattern, both experimentally and by computation. Still the proximity of the high power TV station explains the prevailing practice of using Channel IV antenna for Channel V broadcast.

Table 7 3

Item	Impedance	Gain wr to isotropic			
	Cheng and Chens	Exptal	Cheng and	Exptal	Chens
Initial array	94.71+j74.79	100+j70	01 12 372		11.45
Final array	10.29+j6 10	10+j3	05 21.9		20 08

Table 7.4

Freq MHz	Gain	Gain in dB
	wr to isotropic out	
56	2.73	4.36
57	3.075	4 88
58	3.736	5 725
59	4.753	6.77
60	6 23	7.95
61	8.21	9.14
62	10 57	10 24
63	13 0	11.14
64	15.1	11.79
65	16 08	12.06
66	10 318	10.13
67	4 012	6 03

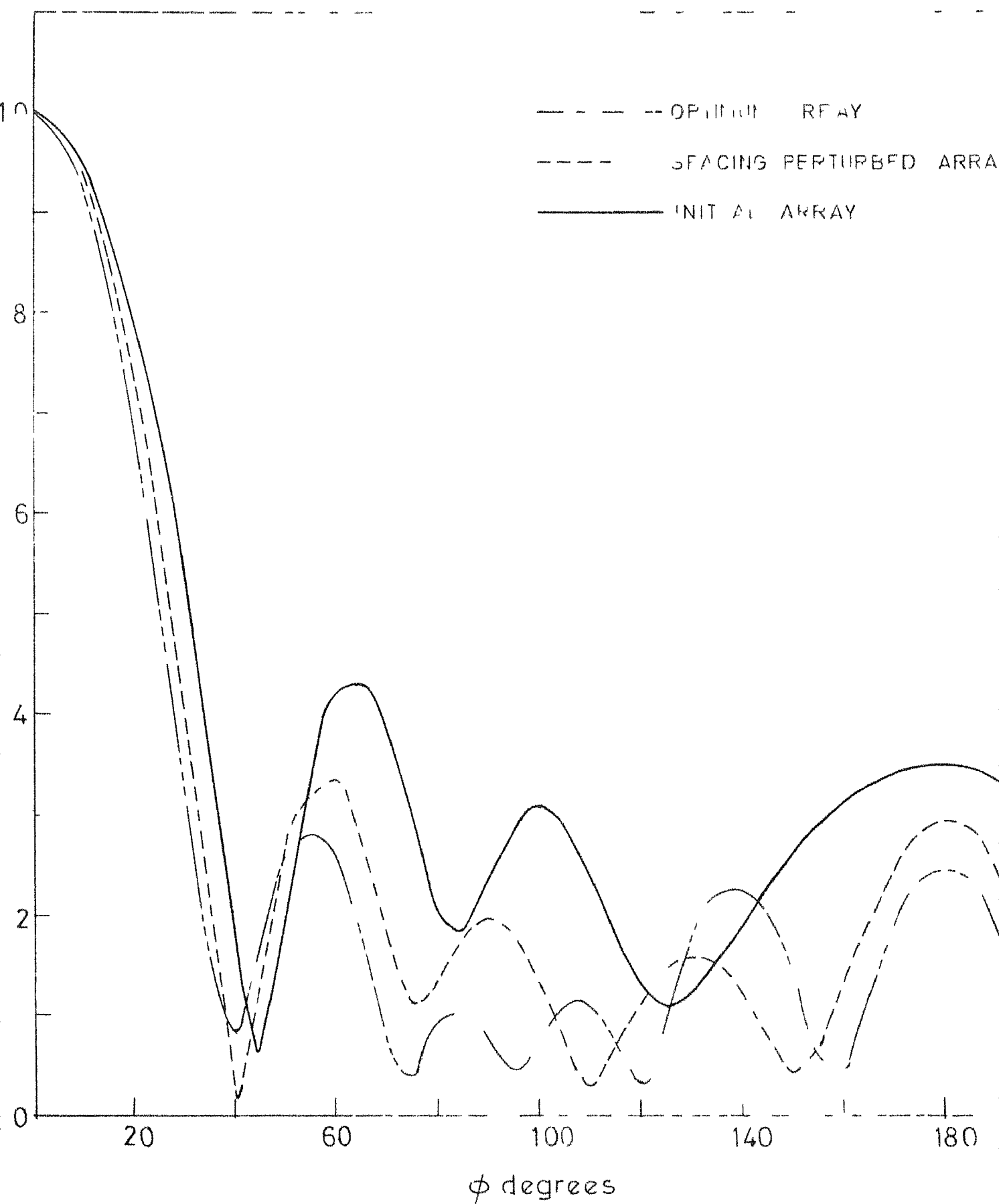


FIG 7 3 COMPARISON OF INITIAL SPACE PERTURBED AND OPTIMIZED PATTERNS

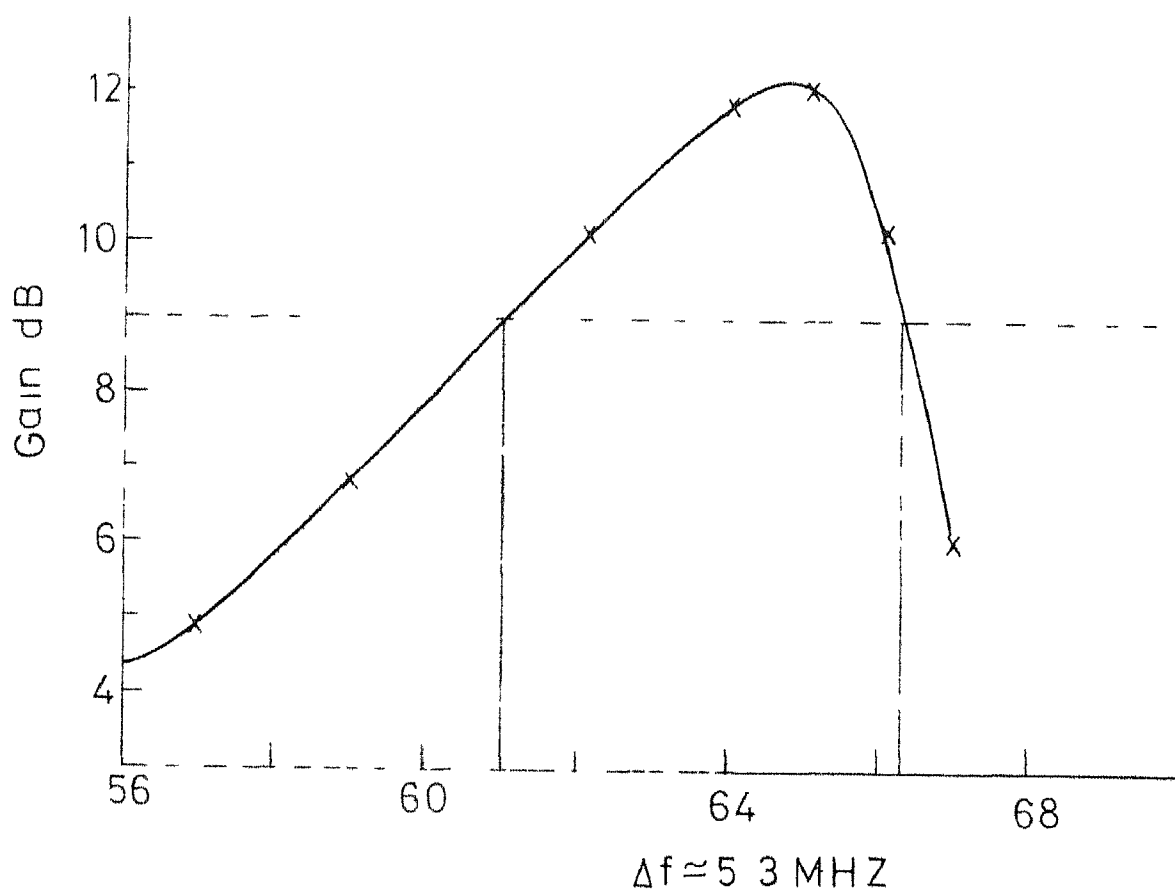


FIG 7 4 BANDWIDTH OF ANTENNA

A study of the increase in gain as the number of directors in a Yagi antenna is increased has also been done and the results are shown in Table 7 6 and plotted in Fig 7.5 These results also agree with the generally held views like the increase in number of directors need not necessarily increase the gain A sort of saturation seems to occur with higher number of directors.

#### 7.4 Conclusion

A computer program which is versatile is developed. Any future analysis can make use of this program. The antenna set up also can be used for future research. The effect of the diameter of the elements as an experimental parameter can also be taken up. Optimization with cost, array size, impedance etc. can be performed with little modification to the computer program.

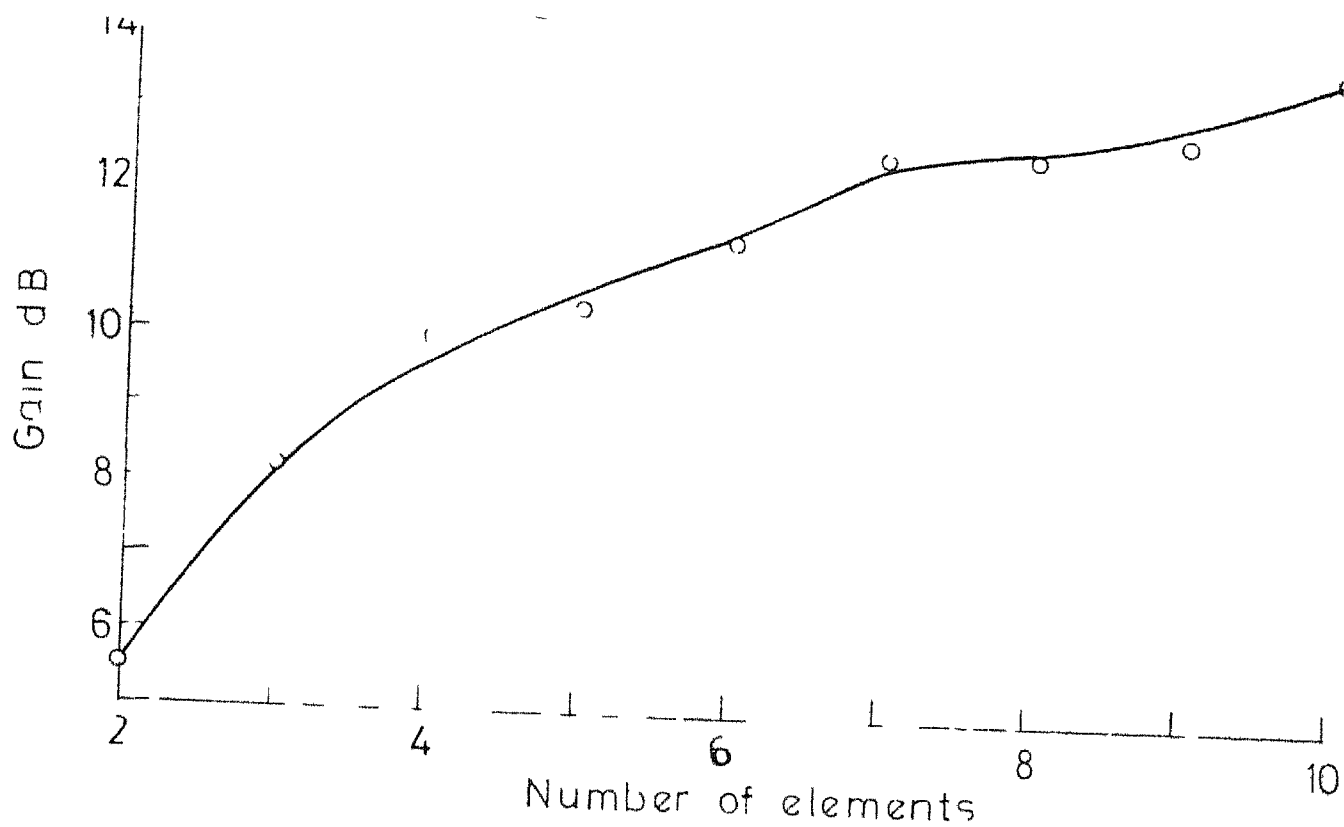


FIG 7 5 GAIN VS NO OF ELEMENTS

Table 7 5

Freq. MHz	Gain wr to isotropic out	Gain in dB
65	12 52	10.98
80	2 726	4 35
95	2 721	4 34
110	2.749	4.393
125	2 76	4.41
140	2.49	3 96
155	2.23	3.5
170	2 40	3.8
185	2.98	4 75
200	3.77	5 77

Table 7.6

Number of elements	Gain wr to isotropic radiator	Gain in dB
2	3.54	5.49
3	6.66	8.23
4	9 97	9.99
5	10.73	10.30
6	13.34	11.25
7	17 74	12.49
8	17 81	12.5
9	18 95	12.77
10	23 83	13.77

APPENDIX I

## DESIGN TABLES FOR YAGI ARRAY

Table I  $b/h = 0.5$ ,  $\lambda$  = free space wavelength

N	$\beta_o h$	DD (dB)	Bandwidth %	Array size ( )
6	1.35	7.6	20.7	0.65
8	1.34	8.7	20.2	0.85
10	1.32	9.6	19.7	1.05
12	1.31	10.3	18.3	1.25
14	1.30	11.0	16.9	1.45
16	1.29	11.4	15.5	1.64
18	1.28	11.9	14.1	1.83
20	1.28	12.4	13.3	2.03
24	1.27	13.3	12.6	2.42
28	1.26	13.9	11.1	2.80
32	1.25	14.5	9.6	3.18
36	1.25	15.0	8.9	3.56
40	1.24	15.5	8.1	3.94
44	1.24	15.8	8.1	4.33
48	1.23	16.0	6.5	4.70
52	1.23	15.9	6.5	5.10
56	1.22	16.2	4.9	5.45
60	1.22	16.0	4.9	5.83



Table II       $b/h = 1.0$ 

N	$\beta_{oh}$	D (dB)	Bandwidth %	Array size ( )
3	1.38	6.8	12.4	0.66
6	1.37	9.9	11.0	1.3
8	1.36	11.3	10.3	1.73
10	1.36	12.5	10.3	2.16
12	1.35	13.3	8.9	2.58
14	1.34	14.0	7.5	2.98
16	1.34	14.7	7.5	3.41
18	1.34	15.1	6.8	3.82
20	1.33	15.6	6.0	4.23
22	1.33	15.9	5.3	4.64
24	1.32	16.3	4.6	5.05
26	1.32	16.5	4.6	5.45
28	1.32	16.6	3.8	5.85
30	1.32	16.4	3.8	6.28

Table III     $b/h = 1.5$ 

N	$\beta_{0h}$	D (dB)	Bandwidth %	Array size ( )
3	1.38	7.9	5.1	4.91
6	1.37	11.1	4.4	1.96
8	1.37	12.7	4.4	2.62
10	1.37	13.8	4.0	3.26
12	1.37	14.8	4.0	3.91
14	1.37	15.6	4.0	4.56
16	1.37	16.1	3.7	5.20
18	1.36	16.5	3.3	5.86
20	1.36	17.0	2.9	6.50

All these values are valid for the First  
pass band  $\beta_{0h} = 0$  to 1.57) and for  $a/h = 0.01$ .

## APPENDIX II

### TWO ELEMENT ARRAY

#### A.1 Integral Equation for two elements

The integral equation (4.27) for the current in a single isolated antenna is generalized to apply to the two identical parallel and non-staggered elements shown in Fig. A 1. It is merely necessary to add to the vector potential on the surface of each element the contributions by the current in the other element. Hence, for element 1, the vector potential difference is

$$\begin{aligned}
 & 4\pi \mu_0^{-1} [A_{1Z}(Z) - A_{1Z}(h)] \\
 &= \int_{-h}^h [I_{1Z}(Z') K_{11d}(Z, Z') + I_{2Z}(Z') K_{12d}(Z, Z')] dZ' \\
 &= \frac{14\pi}{\cos \beta_0 h} \left[ \frac{1}{2} V_{10} \sin \beta_0 (h - |Z|) + U_1 (\cos \beta_0 Z - \cos \beta_0 h) \right] \quad (A.1)
 \end{aligned}$$

Similarly, for element 2

$$\begin{aligned}
 & 4\pi \mu_0^{-1} [A_{2Z}(Z) - A_{2Z}(h)] \\
 &= \int_{-h}^h [I_{1Z}(Z') K_{21d}(Z, Z') + I_{2Z}(Z') K_{22d}(Z, Z')] dZ' \\
 &= \frac{14\pi}{\cos \beta_0 h} \left[ \frac{1}{2} V_{20} \sin \beta_0 (h - |Z|) + U_2 (\cos \beta_0 Z - \cos \beta_0 h) \right] \quad (A.2)
 \end{aligned}$$

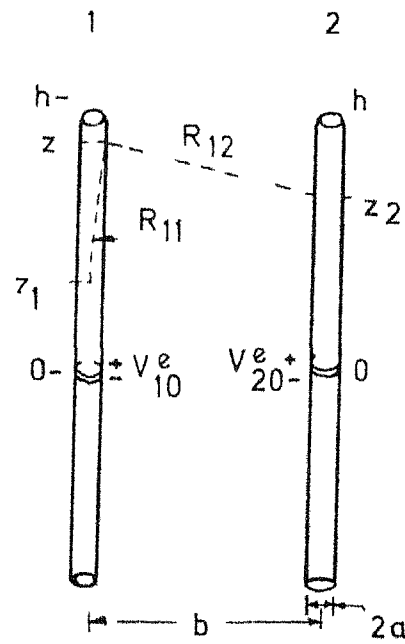


FIG A1 TWO IDENTICAL PARALLEL ANTENNAS

In these expressions

$$\begin{aligned}
 K_{11d}(Z, Z') &= \frac{e^{-j\beta_o R_{11}}}{R_{11}} - \frac{e^{-j\beta_o R_{11h}}}{R_{11h}} \\
 &= K_{11}(Z, Z') - K_{11}(h, Z') \quad (A.3)
 \end{aligned}$$

$$\begin{aligned}
 K_{12d}(Z, Z') &= \frac{e^{-j\beta_o R_{12}}}{R_{12}} - \frac{e^{-j\beta_o R_{12h}}}{R_{12h}} \\
 &= K_{12}(Z, Z') - K_{12}(h, Z') \quad (A.4)
 \end{aligned}$$

with

$$R_{11} = \sqrt{(Z-Z')^2 + a^2}, \quad R_{11h} = \sqrt{(h-Z')^2 + a^2} \quad (A.5)$$

$$R_{12} = \sqrt{(Z-Z')^2 + b^2}, \quad R_{12h} = \sqrt{(h-Z')^2 + b^2} \quad (A.6)$$

$K_{22d}(Z, Z')$  and  $K_{21d}(Z, Z')$  are obtained from the above formulas when 1 is substituted for 2 and 2 for 1 in the subscripts.

The two simultaneous integral equations (A.1) and (A.2) can be reduced to a single equation in two special cases,

- (a) The zero phase sequence when the two driving voltages are identical so that the two currents are the same,
- (b) the first phase sequence when the two deriving voltages and the resulting two currents are equal in magnitude but  $180^\circ$  out of phase. Specifically for the zero phase sequence,

$$V_{10} = V_{20} = V^{(0)}, I_{1Z}(Z) = I_{2Z}(Z) = I_Z^{(0)}(Z) \quad (\text{A.7})$$

so that the equation (A.1) and (A.2) become

$$\begin{aligned} & \int_{-h}^h I_Z^{(0)}(Z') K_d^{(0)}(Z, Z') dZ' \\ &= \frac{j4\pi}{\epsilon_0 \cos \beta_0 h} \left[ \frac{1}{2} V^{(0)} \sin \beta_0 (h - |Z|) + U^{(0)} (\cos \beta_0 Z - \cos \beta_0 h) \right] \end{aligned} \quad (\text{A.8})$$

where

$$U^{(0)} = \frac{-j\epsilon_0}{4\pi} \int_{-h}^h I_Z(Z') K^0(h, Z') dZ' \quad (\text{A.9})$$

and

$$K^{(0)}(Z, Z') = \frac{-j\beta_0 R_{11}}{R_{11}} + \frac{-j\beta_0 R_{12}}{R_{12}} \quad (\text{A.10})$$

$$K_d^{(0)}(Z, Z') = K^{(0)}(Z, Z') - K^{(0)}(h, Z') \quad (\text{A.11})$$

Similarly, for the first phase sequence,

$$V_{10} = -V_{20} = V^{(1)}, I_{1Z}(Z) = -I_{2Z}(Z) = I_Z^{(1)}(Z) \quad (\text{A.12})$$

so that the two equations again become alike and equal to

$$\begin{aligned} & \int_{-h}^h I_Z^{(1)}(Z') K_d^{(1)}(Z, Z') dZ' = \frac{j4\pi}{\epsilon_0 \cos \beta_0 h} \left[ \frac{1}{2} \sin \beta_0 (h - |Z|) \right. \\ & \quad \left. + U^{(1)} (\cos \beta_0 Z - \cos \beta_0 h) \right] \end{aligned} \quad (\text{A.13})$$

where

$$U^{(1)} = \frac{-j\omega_0}{4\pi} \int_{-h}^h I_Z(Z') K^{(1)}(h, Z') dZ' \quad (A.14)$$

and

$$K^{(1)}(Z, Z') = \frac{e^{-j\beta_0 R_{11}}}{R_{11}} - \frac{e^{-j\beta_0 R_{12}}}{R_{12}} \quad (A.15)$$

$$K_d^{(1)}(Z, Z') = K^{(1)}(Z, Z') - K^{(1)}(h, Z') \quad (A.16)$$

A point to note is that the two phase sequences differ only in the sign in  $K^{(0)}(Z, Z')$  and  $K^{(1)}(Z, Z')$ .

If (A.8) can be solved for the zero-phase-sequence current  $I_Z^{(0)}(Z)$  and (A.13) for the first-phase-sequence current  $I_Z^{(0)}(Z)$ , the currents  $I_{1Z}(Z)$  and  $I_{2Z}(Z)$  maintained by the arbitrary voltages  $V_{10}$  and  $V_{20}$  can be obtained simply by superposition. This follows directly if  $V^{(0)}$  and  $V^{(1)}$  are so chosen that

$$V^{(0)} = \frac{1}{2} [V_{10} + V_{20}], \quad V^{(1)} = \frac{1}{2} [V_{10} - V_{20}] \quad (A.17)$$

In this case,

$$V_{10} = V^{(0)} + V^{(1)}, \quad V_{20} = V^{(0)} - V^{(1)} \quad (A.18)$$

so that

$$I_{1Z}(Z) = \cancel{I_Z^{(0)}(Z)} = I_Z^{(0)}(Z) + I_Z^{(1)}(Z)$$

$$I_{2Z}(Z) = I_Z^{(0)}(Z) - I_Z^{(1)}(Z) \quad (A.19)$$

## A.2 Properties of the integrals:

The two integral equations (A.8) and (A.13) for the phase-sequence currents are formally exactly like the equation (4.27) for the isolated antenna. They differ only in the kernels of the integrals on the left and in the definitions (A.9) and (A.14) of the functions  $U$ . Each of these is now the algebraic sum of two terms that are identical except that the radius  $a$  appears in the first term, the distance  $b$  between the elements in the second term. In order to determine the effect of this difference on the current<sup>it</sup> is convenient to consider first the two extreme cases when the elements are very close together and when they are very far apart.

The two elements may be considered close together when  $\beta_0 b \ll 1$  and  $b \ll h$ . In this case, since  $b$  satisfies substantially the same conditions as  $a$ , the behaviour of the integrals that contain  $b$  corresponds closely to that of the integrals that contain  $a$ . When the antennas are so far apart

$(\beta_0 b \gg 1, b \gg h)$  that  $(\beta_0 \sqrt{b^2 + h^2} - \beta_0 b) \ll 1$ , the contribution to the difference kernels  $K_d^{(0)}(z, z')$  by the term  $K_{12}(z, z')$  is very small since  $R_{12}$  and  $R_{12h}$  differ only slightly. In this case, the principal part of the interaction between the currents in the two

$$= \left( e^{-j\beta_0 R_{12}/R_{12}} \right) - \left( e^{-j\beta_0 R_{12h}/R_{12h}} \right)$$



antennas is included in the function  $U^{(0)}$  or  $U^{(1)}$  and the integrals on the left in (A.8) and (A.13) are only slightly different from the corresponding integral for the single antenna. The interaction between the currents in the two antennas is approximately as if each maintained along the other a vector potential that is uniform in amplitude and phase. Accordingly, the current induced in each element by the other is distributed in a first approximation as a shifted cosine. This conclusion follows directly from the fact that the component of current associated with the constant part of the vector potential along the surface of the isolated antenna is distributed in this manner.

When the separation of the two elements is such that  $\beta_0 b > 1$  but not so great that  $\beta_0 \sqrt{b^2 + h^2}$  differs negligibly from  $\beta_0 b$ , the vector potentials maintained by the currents on the one antenna at points along the surface of the other differ significantly from one another in phase due to retarded action. The induced currents should then have two components, the one distributed approximately as the shifted cosine with half-angle arguments, the other as the shifted cosine.

In order to verify the correctness of these conclusions the difference integral

$$S_b(h, Z) - S_b(h, h) = \int_{-h}^h \sin \beta_0 |Z'| K_d(Z, Z') dZ' \quad (A.20)$$

has been evaluated for  $\beta_0 h = \pi$  over a range of values of  $\beta_0 b$  extending from 0.04 to 4.5. The real and imaginary parts are shown in Fig. A.2 together with the three trigonometric functions,  $\sin \beta_0 Z$ ,  $(\cos \beta_0 Z + 1)$  and  $\cos \frac{1}{2} \beta_0 Z$ , to which the sine, shifted cosine and shifted cosine with half-angle arguments reduce when  $\beta_0 h = \pi$ . For convenience in the graphical comparison -  $(\cos \beta_0 Z + 1)$  and  $-\cos \frac{1}{2} \beta_0 Z$  are shown. It is evident from Fig. A.2 that the real part of the difference integral approximates  $\sin \beta_0 Z$  when  $\beta_0 Z < 1$ ,  $1 + \cos \beta_0 Z$  when  $\beta_0 b \geq 1$ . On the other hand, the imaginary part resembles the shifted cosine with half-angle arguments, in this case  $\cos \frac{1}{2} \beta_0 Z$ , for all values of  $\beta_0 b$ .

As a consequence of these observations, the following approximate representation of the integrals in (A.8) and (A.13) is indicated:

For  $\beta_0 b < 1$ ,

$$\begin{aligned} \int_{-h}^h I_Z(Z') \left( \frac{\cos \beta_0 R_{12}}{R_{12}} - \frac{\cos \beta_0 R_{12h}}{R_{12h}} \right) dZ' \\ = \Psi_{12}(Z) I_Z(Z) = \Psi_{12} I_Z(Z) \end{aligned} \quad (A.20a)$$

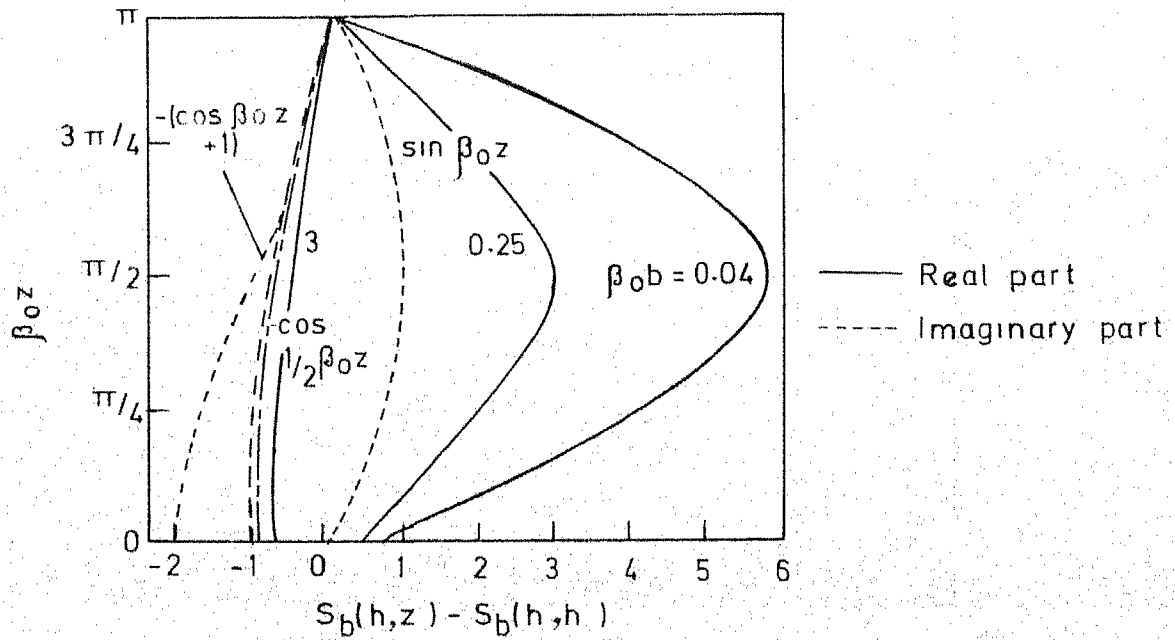


FIG. A2 THE FUNCTIONS  $S_b(h, z) - S_b(h, h)$  COMPARED WITH THREE TRIGONOMETRIC FUNCTIONS

where  $\psi_{12}$  is a constant,

For  $\beta_0 b \gg 1$ ,

$$\int_{-h}^h I_Z(Z') \left( \frac{\cos \beta_0 R_{12}}{R_{12}} - \frac{\cos \beta_0 R_{12h}}{R_{12h}} \right) dZ',$$

$$r_V \cos \beta_0 Z - \cos \beta_0 h. \quad (\text{A.20b})$$

For all values of  $\beta_0 b$

$$\int_{-h}^h I_Z(Z') \left( \frac{\sin \beta_0 R_{12}}{R_{12}} - \frac{\sin \beta_0 R_{12h}}{R_{12h}} \right) dZ',$$

$$r_V \cos \frac{1}{2} \beta_0 Z - \cos \frac{1}{2} \beta_0 h. \quad (\text{A.20c})$$

# APPENDIX III COMPUTER PROGRAMME

Equations used in the programme are

$$W_{KiV}(Z_k) = \int_{-h_i}^{h_i} M_{oZi}(Z'_i) K_{kid}(Z_k, Z'_i) dZ'_i = \sin \beta_o h_i$$

$$[C_{b_{ki}}(h_i, Z_k) - C_{b_{ki}}(h_i, h_k)] - \cos \beta_o h_i [S_{b_{ki}}(h_i, Z_k) - S_{b_{ki}}(h_i, h_k)]$$

$$W_{KiU}(Z_k) = C_{b_{ki}}(h_i, Z_k) - C_{b_{ki}}(h_i, h_k) - \cos \beta_o h_i [E_{b_{ki}}(h_i, Z_k) - E_{b_{ki}}(h_i, h_k)]$$

$$\text{and } W_{KiD}(Z_k) = H_{b_{ki}}(h_i, Z_k) - H_{b_{ki}}(h_i, h_k) - \cos \frac{1}{2} \beta_o h_i [E_{b_{ki}}(h_i, Z_k) - E_{b_{ki}}(h_i, h_k)]$$

where

$$S_b(h, Z) = \int_{-h}^h \sin \beta_o Z' \left[ \frac{e^{-j\beta_o R_1}}{R_1} \right] dZ'$$

$$= \int_0^h \sin \beta_o Z' \left[ \frac{e^{-j\beta_o R_1}}{R_1} + \frac{e^{-j\beta_o R_2}}{R_2} \right] dZ'$$

$$C_b(h, Z) = \int_{-h}^h \cos \beta_o Z' \left[ \frac{e^{-j\beta_o R_1}}{R_1} + \frac{e^{-j\beta_o R_2}}{R_2} \right] dZ'$$

$$H_b(h, Z) = \int_0^h \cos \frac{1}{2} \beta_o Z' \left[ \frac{e^{-j\beta_o R_1}}{R_1} + \frac{e^{-j\beta_o R_2}}{R_2} \right] dZ'$$

$$\text{and } E_b(h, Z) = \int_0^h \left[ \frac{e^{-j\beta_o R_1}}{R_1} + \frac{e^{-j\beta_o R_2}}{R_2} \right] dZ'$$

$$\text{where } R_1 = \sqrt{(Z-Z')^2 + b_{ki}^2}$$

$$\text{and } R_2 = \sqrt{(Z+Z')^2 + b_{ki}^2}$$

```

39  CONTINUE
DO 37 I=2,N
  I=I-1
  WRITE (10,100) I, I, YY(I)
923  ***** SAVING BETWEEN ELEMENTS 'I1,' AND 'I1, '=', F10.
  5, '*****')
37  CONTINUE
C*****
C  CREATION OF SAVING MATRIX
C
DO11 I=1,N
  SUM=0.0
DO11 J=1,N
  IF(I-J) 12,13,14
12  S(I,J)=YY(J)+SUM
  SUM=S(I,I)
  GO TO 11
13  S(I,J)=YY(I)
  GO TO 11
14  S(I,J)=S(I,I)
11  CONTINUE
  WRITE (10,1)
  WRITE (10,100)
  FORMAT(' SAVING MATRIX')
  WRITE (10,1)
  WRITE (10,110), ((S(I,J), J=1,N), I=1,N)
110  FORMAT(10,5F10.7)
C*****
C  TO FIND THE FREQUENCY DEPENDANCE OF THE STRUCTURE
DO 10001 LF=65,200,15
  LAMBDA=300./LF
  WRITE (10,403), LF, LAMBDA
403  FORMAT(10, 'FREQ.=', 2X, 13, 2X, 'WZ', 2X, 'WAVE LENGTH =', F10.4, 2X
  5, 'WZTRES')
C*****
C  CREATION OF Z MATRIX
C
DO 15 J=1,N
  DEL=2.*H(J)/(N-1)
  Y=H(J)+DEL
DO15 I=1,21
  Z(I,J)=Y-DEL
15  Y=Z(I,J)
  M1=(N-1)/2.+1
C
C  CREATION OF S(L,I,J) MATRICES
C
DO16 L=1,9
DO16 J=1,9
DO16 I=1,M1
  RH(L,I,J)=SQRT(Z(I,J)**2+S(L,J)**2)
  RH(L,I,J)=SQRT((H(L)-Z(I,J))**2+S(L,J)**2)
  RH2(L,I,J)=SQRT((H(L)/2.-Z(I,J))**2+S(L,J)**2)
  RHP(L,I,J)=SQRT((H(L)+Z(I,J))**2+S(L,J)**2)
  RH2P(L,I,J)=SQRT((H(L)/2.+Z(I,J))**2+S(L,J)**2)
C
C  PRELIM TO INTEGRATION

```

```

PI=4.*ATAN(1.)
BO=2.*PI/LAMBDA
WRITE (IU,1)
WRITE(IU,4),BO
FORMAT(1H0,'WAVE NUMBER=',F10.4)
WRITE (IU,1)
E=(0.0,1.0)

```

# NUMERICAL INTEGRATION USING SIMSON'S RULE

```

DO17 L=1,N
DO17 J=1,M
DO17 I=1,M1
EZ0(L,I,J)=2*EXP(-E*BO*RH(L,I,J))/RH(L,I,J)
SZ0(L,I,J)=SIN(BO*Z(I,J))*EZ0(L,I,J)
CZ0(L,I,J)=COS(BO*Z(I,J))*EZ0(L,I,J)
HZ0(L,I,J)=COS(0.5*BO*Z(I,J))*EZ0(L,I,J)
CALL SIMSON(SZ0,SBH20)
CALL SIMSON(CZ0,CBH20)
CALL SIMSON(HZ0,HBH20)
DO 17771 L=1,N
DO 17771 J=1,M
DO 17771 I=1,M1
EZ0(L,I,J)=EXP(-E*BO*RH2(L,I,J))/RH2(L,I,J)+EXP(-E*BO*RH2P(L,I,J))/RH2P(L,I,J)
SZ0(L,I,J)=SIN(BO*Z(I,J))*EZ0(L,I,J)
CZ0(L,I,J)=COS(BO*Z(I,J))*EZ0(L,I,J)
17771 HZ0(L,I,J)=COS(0.5*BO*Z(I,J))*EZ0(L,I,J)
CALL SIMSON(SZ0,SBH2H2)
CALL SIMSON(CZ0,CBH2H2)
CALL SIMSON(HZ0,HBH2H2)
DO 1771 L=1,N
DO 1771 J=1,M
DO1771 I=1,M1
EZ0(L,I,J)=EXP(-E*BO*RH(L,I,J))/RH(L,I,J)+EXP(-E*BO*RH2(L,I,J))/RH2(L,I,J)
SZ0(L,I,J)=SIN(BO*Z(I,J))*EZ0(L,I,J)
CZ0(L,I,J)=COS(BO*Z(I,J))*EZ0(L,I,J)
1771 HZ0(L,I,J)=COS(0.5*BO*Z(I,J))*EZ0(L,I,J)
CALL SIMSON(SZ0,SBH2)
CALL SIMSON(CZ0,CBH2)
CALL SIMSON(HZ0,HBH2)
DO 17777 L=1,N
DO17777 J=1,M
DO 17777 I=1,M1
RH(L,I,J)=EZ0(L,I,J)
RH2(L,I,J)=SZ0(L,I,J)
RH2P(L,I,J)=CZ0(L,I,J)
RHPP(L,I,J)=HZ0(L,I,J)
EZ0(L,I,J)=SIN(BO*H(J))*RH2P(L,I,J)+COS(BO*H(J))*RH2(L,I,J)
SZ0(L,I,J)=-COS(BO*H(J))*RH(L,I,J)+RH2P(L,I,J)
17777 CZ0(L,I,J)=-COS(0.5*BO*H(J))*RH(L,I,J)+RHPP(L,I,J)
CALL SIMSON(EZ0,SY)
CALL SIMSON(SZ0,SO)
CALL SIMSON(CZ0,SO)

```

CALCULATION OF  $\psi$ 'S

```

C
DO 5 J=1,N
DO 5 I=1,N
WVO(I,J)=SIN(BO*H(J))*(CBHZO(I,J)-CBHH(I,J))-COS(BO*H(J))*
1(SBHZO(I,J)-SBHH(I,J))
WVH2(I,J)=SIN(BO*H(J))*(CBHZN2(I,J)-CBHH(I,J))-COS(BO*H(J))*
2(SBHZN2(I,J)-SBHH(I,J))
WUO(I,J)=(CBHZO(I,J)-CBHH(I,J))-COS(BO*H(J))*(EBHZO(I,J)-EBHH(I
1,J))
WUH2(I,J)=(CBHZN2(I,J)-CBHH(I,J))-COS(BO*H(J))*(EBHZN2(I,J
2)-EBHH(I,J))
WDO(I,J)=(HBHZO(I,J)-HBHH(I,J))-COS(BO*H(J)*0.5)*(EBHZO(I,J)
3-FBHH(I,J))
WDH2(I,J)=(HBHZN2(I,J)-HBHH(I,J))-COS(0.5*BO*H(J))*(FBHZN2(I,J)
4-FBHH(I,J))

```

# GENERATION OF PSI MATRICES

```

C
DO 18 I=1,N
DELTA1(I)=SIN(BO*H(I))*(COS(BO*H(I)/4.))-COS(BO*H(I)/2.))-
1SIN(BO*H(I)/2.))*((1.-COS(BO*H(I)/2.))
18 DELTA2(I)=(1.-COS(BO*H(I)))*(COS(BO*H(I)/4.))-COS(BO*H(I)/2.))
2-(COS(BO*H(I)/2.))-COS(BO*H(I)))*((1.-COS(BO*H(I)/2.))
SHDV22=(1./DELTA1(2))*(WVO(1,2)*(COS(BO*H(2)/4.))-COS(BO*H(2)/2.
1))-WVH2(2,2)*(1.-COS(BO*H(2)/2.))

```

```

V=1.0
A2=E*V/(60*SHDV22*COS(BO*H(2)))
WRITE(T0,131) A2
131 FORMAT(150,'A2=',F10.4,3X,' ',F10.4)
C
WRITE(10,1)
DO 19 J=1,N
SHDV2(I)=(1./DELTA2(I))*(WVO(1,2)*(COS(BO*H(I)/4.))-COS(BO*H(I)
1/2.))-WVH2(1,2)*(1.-COS(BO*H(I)/2.))
SHDV2(2)=(0.0,0.0)
DO 20 I=1,N
SHDV2(I)=(1./DELTA2(I))*(WVH2(1,2)*(1.-COS(BO*H(I))) - WVO(1,2)
20 6*(COS(BO*H(I)/2.))-COS(BO*H(I)))
SHDV2(2)=(1./DELTA1(2))*(WVH2(2,2)*SIN(BO*H(2))-WVO(2,2)*
6SIN(BO*H(2)/2.))
DO 21 I=1,N
AA=COS(BO*H(I)/4.))-COS(BO*H(I)/2.))
BB=1.-COS(BO*H(I)/2.))
CCC=COS(BO*H(I)/2.))-COS(BO*H(I))
DD=1.-COS(BO*H(I))
DO 21 J=1,N
SHDU(I,J)=(1./DELTA2(I))*(WDO(I,J)*AA-WUH2(I,J)*BB)
SHDU(I,J)=(1./DELTA2(I))*(WUH2(I,J)*DD-WDO(I,J)*CCC)
SHDU(I,J)=(1./DELTA2(I))*(WDO(I,J)*AA-WUH2(I,J)*BB)
SHDU(I,J)=(1./DELTA2(I))*(WUH2(I,J)*DD-WDO(I,J)*CCC)

```

# GENERATION OF PHI MATRICES

```

C
DO 22 J=1,N
DEL2(I)=0.0
DEL2(2)=1.0
DO 23 I=1,N
PHI2V(I)=SV(I,2)-(1.-DEL2(I))*SHDV2(I)*COS(BO*H(I))
DO 24 J=1,N
DO 24 I=1,N
PHIU(I,J)=SU(I,J)-SHDU(I,J)*COS(BO*H(I))

```



```

24 PHID(I,J)=SD(I,J)-SFDD(I,J)*COS(B0*H(I))
C
C
C CREATION OF XX,ZZ MATRICES
DO30 J=1,N
30 ZZ(J)=-PHI2V(J)*A2
J=N
DO31 K=1,N
31 ZZ(J+K)=-SHDV2(K)*A2
DO32 J=1,N
DO32 I=1,M
32 XX(I,J)=PHIU(I,J)
J=N
DO33 K=1,N
DO33 L=1,M
33 XX(L,J+K)=PHID(L,K)
L=M
DO34 MM=1,N
DO34 LL=1,M
34 XX(M+L,MM)=SFDD(MM,LL)
MM=N
MM=N
DO35 LL=1,N
DO35 KK=1,M
35 XX(M+KK,MM+LL)=SFDD(KK,LL)
M1=2*N
CALL MATINV(XX,M1,ZZ,DETERM,I0)
DO 400 I=1,M
400 C(I)=ZZ(I)
DO401 I=M+1,M1
401 D(I-M)=ZZ(I)
C
WRITE(I0,919),DETERM
919 FORMAT(100,'DETERMINANT=',F10.4,2X,F10.4)
WRITE(I0,4),I0
C
WRITE(I0,1)
C
WRITE(I0,395)
395 FORMAT(15X,'REAL',15X,'IMAGINARY')
DO36 I=1,M
C
WRITE(I0,99),I,C(I)
C
99 FORMAT(140,'B(',I1,')',5X,F10.4,5X,F10.4)
36 CONTINUE
C
C CURRENT MATRIX
C
DO 50 J=1,N
DO50 I=1,21
50 CUR(I,J)=C(J)*(COS(B0*Z(I,J))-COS(B0*H(J)))+D(J)*(COS(0.5*B0*
6Z(I,J))-COS(0.5*B0*H(J)))
DO 554 I=1,21
554 CUR(I,2)=CUR(I,2)+A2*(SIN(B0*(H(2)-Z(I,2))))
C
WRITE(I0,1)
C
WRITE(I0,551)
551 FORMAT(100,'THE CURRENT DISTRIBUTION IN YAGI ANTENNA')
C
WRITE(I0,552),((CUR(I,J),J=1,N),I=1,41)
552 FORMAT(140,2(1X,F10.4,F10.4))
YIN=CUR(21,2)/V
ZIN=1/YIN
WRITE(I0,1)
WRITE(I0,40),YIN
40 FORMAT(140,'THE INPUT ADMITTANCE=',F10.4,2X,',',F10.4)

```

```

42 WRITE (IU,42),ZIN
   FORMAT(1H0,'TH INPUT IMPEDANCE =',F10.4,2X,'.',F10.4)
   WRITE (IU,1)
C
C CALCULATION OF E FIELD AND PATTERN IN  $\theta=90$  DEGREES PLANE
C
CALL KANSO(COR,R)
WRITE(IU,*), (C(I),I=1,N)
D1=-5.
DO 555 I=1,73
  DG(I)=5+D1
559 P1=DG(I)
  DO 556 K=1,37
    EFIELD(K)=CEXP(-E*BO*S(1,2)*COSD(DG(K)))*R(I)
  DO 669 I=2,N
    EFIELD(K)=EFIELD(K)+CEXP(E*BO*S(2,I)*COSD(DG(K)))*R(I)
669 CONTINUE
556 WRITE(IU,578), (EFIELD(I),I=1,37)
578 FORMAT(1H0,'EFIELD WITH  $\theta=90$ DEG',/3(1X,F10.4,2X,F10.4))
  DO 601 I=1,37
    F1(I)=CABS(EFIELD(I))
    T(I)=ATAN(AIMAG(EFIELD(I))/REAL(EFIELD(I)))
    IF(REAL(EFIELD(I)).LT.0.0) T(I)=T(I)+PI
    IF(T(I).LT.0.0) T(I)=T(I)+PI*2.
    T(I)=T(I)*(180/PI)
601 CONTINUE
    A*AX=F1(I)
    DO 414 I=1,37
      IF(F1(I).GE.AMAX) GO TO 1223
    GO TO 414
1223 AMAX=F1(I)
    K1=I
    CONTINUE
414 WRITE(IU,908),EFIELD(K1)
908 FORMAT(1H0,'MAX.EFIELD=',F10.4,1X,'.',F10.4)
    P1=(K1-1)*5
    WRITE(IU,909),K1
909 FORMAT(1H0,'IN THETA= 90 DEG & PHI=',2X,I3,'DEG')
    DO 415 I=1,37
      F1(I)=F1(I)/AMAX
    WRITE (IU,557)
557 FORMAT(1H0,'PHI',15X,'EFIELD WITH THETA=90DEGREES',10X,'PHASE')
    WRITE(IU,1)
    DO 600 I=1,37
      WRITE(IU,558),DG(I),F1(I),T(I)
558 FORMAT(1X,'.',5X,F8.3,5X,'.',5X,F10.4,5X,'.',11X,F10.5,12X,'*')
600 CONTINUE
    WRITE(IU,1)
C
C CALCULATION OF DIRECTIVITY
C
CALL PINPUT(COR,PIS,DG,EF,SC,Z,5)
WRITE(IU,*), (EF(1,K),K=1,73)
WRITE (IU,888),PIS
888 FORMAT(1H0,'INPUT POWER=',5X,E15.8)
    MAX=0.0
    DO 6543 I=1,73
      DO 6543 J=1,37
        IF(CABS(MAX).LT.CABS(EF(I,J))) GO TO 9087
      GO TO 6543

```

```

9087 MAX=500000
K2=(1-1)
K3=(1-1)
6543 CONTINUE
WRITE(10,100) MAX
798 FORMAT(100,'AX,E FIELD=',F10.4,2X,F10.4)
799 WRITE(10,100) K2,K3
WRITE(10,100) 'IN THE DIRECTION THETA=',2X,I3,'DEG',2X,'PHI=',
52X,I3,'DEG'
GAIN(1)=(2*PI*(MAX)**2)/(60.*PIN)
WRITE(10,100) GAIN(1)
3115 FORMAT(100,'GAIN',F10.6)
GAIN(1)=10.*ALOG10(GAIN(1))
WRITE(10,545) GAIN(1)
545 FORMAT(100,'DIRECTIVITY =',F10.6,'DB')
WRITE(10,1)
10001 CONTINUE
CLOSE(UNIT=10,FILE='OUT.FOR')
STOP
END

```

```

C
C THIS SUBROUTINE INVERTS THE MATRIX 'XX'
C
SUBROUTINE INVERT(A,N,DET,PIVOT,ICOL)
DIMENSION INDEX(20,3),A(20,20),C(20)
EQUIVALENCE (IR,JR),(ICOL,JCOL)
COMPLEX A,B,DETERM,SWAP,PIVOT,X
DETERM=(1.0,0.0)
N=N1
DO 100J=1,N
INDEX(J,3)=0.0
DO 400I=1,N
AMAX=0.0
DO 400K=1,N
IF(INDEX(J,3).EQ.1)GO TO 40
DO 30K=1,N
IF(INDEX(K,3)-1)20,30,115
20 IF((AMAX).GE.CABS(A(J,K)))GO TO 30
IR=J
ICOL=K
AMAX=CABS(A(J,K))
CONTINUE
CONTINUE
INDEX(ICOL,3)=INDEX(ICOL,3)+1
INDEX(I,1)=IR
INDEX(I,2)=ICOL
IF(IR.EQ.ICOL)GO TO 60
DETERM=-DETERM
DO 50L=1,N
SWAP=A(IR,L)
A(IR,L)=A(ICOL,L)
A(ICOL,L)=SWAP
SWAP=B(IR)
B(IR)=B(ICOL)
B(ICOL)=SWAP
60 PIVOT=A(ICOL,ICOL)
DETERM=DETERM*PIVOT
A(ICOL,ICOL)=(1.0,0.0)
DO 70L=1,N
A(ICOL,L)=A(ICOL,L)/PIVOT
70

```

```

      B(ICOLUMN)=B(ICOLUMN)/PIVOT
      DO 90 I=1,N
      IF (I1.EQ.ICOLUMN) GO TO 90
      T=A(I1,ICOLUMN)
      A(I1,ICOLUMN)=(0.0,0.0)
      DO 80 J=1,N
      A(I1,J)=A(I1,J)-A(ICOLUMN,J)*T
      B(J)=B(J)-B(ICOLUMN)*T
90    CONTINUE
      DO 110 I=1,N
      L=N-I+1
      IF (INDEX(L,1).EQ.INDEX(L,2)) GO TO 110
      JROW=INDEX(L,1)
      JCOLUMN=INDEX(L,2)
      DO 100 K=1,N
      SWAP=A(K,JROW)
      A(K,JROW)=A(K,JCOLUMN)
      A(K,JCOLUMN)=SWAP
100   CONTINUE
110   DO 120 K=1,N
      IF (INDEX(K,3).EQ.1) GO TO 120
      ID=2
      RETURN
120   CONTINUE
      ID=1
      RETURN
      END

```

CC THIS SUBROUTINE INTEGRATES SZO ETC. PRELIMINARY TO CALCULATION OF P'S

```

SUBROUTINE SI*SZO(SZO,SBHZO)
COMPLEX SZO,SBHZO,P,PP
DIMENSION B(10),SZO(10,25,10),SBHZO(10,10)
COMMON N,M,H
DO25 I=1,N
DO25 J=1,M
DELL=2.*H(J)/(M-1)
P=(0.0,0.0)
PP=(0.0,0.0)
M1=(M-1)/2
DO261 I=2,M1,2
261 P=SZO(I,I,J)+P
DO 26 I=3,M1,2
26 PP=SZO(I,I,J)+PP
25 SBHZO(I,J)=(DELL/3.)*(SZO(I,1,J)+4.*P+2.*PP+0.5*SZO(I,M1+1,J))
RETURN
END

```

CC THIS SUBROUTINE INTEGRATES THE CURRENT IN THE ELEMENTS

```

SUBROUTINE KANSON(A,B)
COMPLEX A,B,P,PP
COMMON N,M,H
DIMENSION A(25,10),B(10),H(10)
DO 1 J=1,M
DELL=2.*H(J)/(M-1)
P=0.0;PP=0.0
M1=(M-1)/2+1
DO 2 I=2,M1,2
2 P=A(I,J)+P

```

```

DO3 I=3,20,2
PP=A(1,J)+PP
B(J)=(2.*DEL/3.)*(A(1,J)+4.*P+2*PP+0.5*A(21,J))
RETURN
END

```

TO INTEGRATE THE ENTIRE RADIATED FIELD AND TO FIND THE INPUT POWER

```

SUBROUTINE INPUT(CUR,PIN,DG,EF,BD,Z,S)
DIMENSION CUR(25,10),H(10),Z(25,10),DG(80),A1(40,25,10),A21
A(40,10),B(40,80),A4(80),A3(40,80),S(10,10)
COMMON N,M,DEL
COMPLEX A1,A21,EF,E
P=(0.0,0.0)
DO 1 L=1,37
DO 1 J=1,10
DO 1 I=1,10
1 A1(L,I,J)=CUR(I,J)*CEXP(E*BD*Z(I,J)*COSD(DG(L)))*SIND(DG(L))
CALL BHIMA(A1,A21)
DO 2 K=1,73
DO 2 J=1,37
EF(L,K)=CEXP(-P*BD*S(1,2)*SIND(DG(L))*COSD(DG(L)))*A21(L,1)
DO 2 J=2,10
2 EF(L,K)=CEXP(E*BD*S(2,J)*SIND(DG(L))*COSD(DG(L)))*A21(L,J)+EF(L,
4K)
DO 6 K=1,73
DO6 I=1,37
6 A3(L,K)=((CABS(EF(L,K)))**2)*SIND(DG(L))
CALL DELILA(A3,A4)
CALL SAMSON(A4,A5)
PIN=A5/(240.*4.*APAR(1.))
RETURN
END

```

SUBROUTINE BHIMA(A1,A21)

```

COMPLEX A1(40,25,10),A21(40,10),P,PP
DIMENSION B(10)
COMMON N,M,DEL
DO 1 L=1,37
DO 1 J=1,10
DEL=2.*B(J)/(M-1)
P=0.0;PP=0.0
M1=(M-1)/2
DO 2 I=2,M1,2
2 P=P+A1(L,I,J)
DO 3 I=3,M1,2
3 PP=PP+A1(L,I,J)
1 A21(L,J)=(2.*DEL/3.)*(A1(J,1,J)+4.*P+2.*PP+0.5*A1(L,21,J))
RETURN
END

```

SUBROUTINE DELILA(A3,A4)

```

DIMENSION A3(40,80),A4(80)
DEL=(4.*APAR(1.))/36.
DO 1 K=1,73
P=0.;PP=0.
DO 3 L=2,36,2
3 P=P+A3(L,K)

```

```

2 DO 2 L=3,36,2
1 PP=PP+A3(L,K)
A4(K)=(DEL/3.)*(A3(1,K)+4.*P+2.*PP+A3(37,K))
RETURN
END
C
C SUBROUTINE SAWSON(A4,A5)
C
C DIMENSION A4(80)
C DEL=(8.*ATAN(1.))/72.
C P=0.;PP=0.
1 DO 1 K=2,72,2
P=P+A4(K)
2 DO 2 K=3,72,2
PP=PP+A4(K)
A5=(DEL/3.)*(A4(1)+4*P+2*PP+A4(73))
RETURN
END

```

# REFERENCES

1. W.K. Kahn, "Currents on generalized Yagi Structures", IEEE Trans Antennas Propagation, AP 27, Nov 1979, pp 788-797
2. S Uda, "Short wave projector - Historical Record of my studies in Early days", printed privately, Japan, 1974, Ch 1.
3. H Yagi, "Beam transmission of Ultra short waves", Proc IRE, vol. 16, pp. 715-741, June, 1928
4. W Walkinshaw, "Theoretical treatment of short Yagi aeriols", J IEE (London), vol 93, pt III A, No 3, pp. 598-614, 1946
5. D G Reid, "The gain of an idealized Yagi array", J IEE (London), vol 93, pt III A, No 3, pp 564-566, 1946.
6. R M Fishenden and E.A. Wublin, "Design of Yagi aeriols", Proc IEE (London), vol 96, pp 5-12, March, 1949
7. H W Ehrensbeck and H Poehler, "A new method for obtaining maximum gain for Yagi antennas", IRE Trans Antennas Propagation, vol AP-7, pp. 379-386, Oct, 1959
8. D L Sengupta, "On the phase velocity of wave propagation along an infinite Yagi Structure", IRE Trans Antennas Propagation, vol AP-7, pp 234-239, July, 1959
9. F Serracchioli and C A Lewis, "The calculated phase velocity of long end fire dipole arrays", IRE Trans Antenna Propagation, vol AP-7, pp S424-S434, Dec. 1959.
10. L C Shen, "Characteristics of propagating waves on Yagi-Uda structure", IEEE Trans Microwave Theory Tech., vol MTT-19, pp 536-542. June, 1971

11. P.J Mailloux, "Excitation of a surface wave along an infinite Yagi-Uda array", IEEE Trans Antenna Propagation, vol AP-13, pp 719-724, Sept, 1965.
12. R J Mailloux, "The long Yagi-Uda array", IEEE Trans Antennas Propagation, vol AP-14, pp. 128-137, March, 1966
13. J H Bojlsen, H Schjaer-Jacobsen, E Nilsson, and J B Andersen, "Maximum gain of Yagi-Uda arrays", Electronics Letter, vol 7, No 18, pp. 531-532, Sept 9, 1971.
14. I L Morris, Optimization of the Yagi array, Ph D Thesis, Harward University, Cambridge, Mass , 1965
15. F I Tseng and D K Cheng, "Spacing perturbation techniques for array optimization", Radio Sci., vol 3 (New Series), pp. 451-457, May, 1968
16. R W P King, R B Mack, and S S Sandler, Arrays of Cylindrical Dipoles, New York Cambridge, 1968.
17. R F Harrington, Field Computation by Moment Methods, New York MacMillan, 1968
18. D.K Cheng and C A Chen, Optimum element spacing for Yagi-Uda Arrays, Technical Report, TR-72-9, November, 1972, Electrical and Computer Engg Dept , Syracuse University, N Y.
19. C A Chen and D K Cheng, "Optimum element lengths for Yagi-Uda arrays", IEEE Transactions Antennas Propagation, vol. AP-23, No. 1, January, 1975
20. Liang Chi Shen, "Directivity and Bandwidth of single band and double band Yagi arrays", IEEE Trans , Antennas and Propagation, AP 20, pp 778-780, 1972.
21. L C Shen, "Numerical analysis of wave propagation on a periodic linear array", IEEE Trans , Antenna and Propagation, AP-19, pp 289-292, March, 1971.



- 22 D Kajfez , "Non linear optimization reduces the side lobes of Yagi antenna", IEEE Trans , Antenna and Propagation, AP-21, pp 714-715, Sept ,1973
- 23 Nabil K Takla and L.C Shen, "Bandwidth of an Yagi array with optimum directivity", IEEE transactions Antenna and propagation, AP-25, pp 913-914, Nov ,1977.
24. G A Thiele, "Analysis of Yagi-Uda type antenna", IEEE Trans , Antenna and Propagation, AP-17, pp 24-31, January,1969
- 25 J D Kraus, "Antennas", McGraw Hill Book Company, Inc , 1950
- 26 Termen and Petit, "Electronic Measurements", McGraw Hill Book Company, Inc ,1952
- 27 G.A.Thiele, "Computer techniques for electromagnetics" Pergamon Press, Oxford,1973
28. H Jasik, "Antenna Engineering Handbook", McGraw Hill Book Company, Inc , 1961
- 29 E Molloy, "Television Engineers Servicing Manual", George Newnes Limited, Tower House, London, 1952.
- 30 Hewlet Packard Application Note 77-3, Measurement of Complex Impedance.